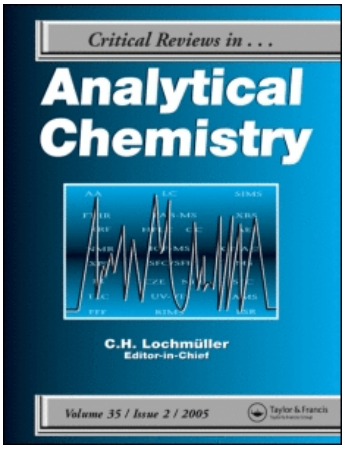

Critical Reviews in Analytical Chemistry
Publication details, including instructions for authors and subscription information:
http://www.informaworld.com/smpp/title~content=t713400837

A Review of CE Detection Methodologies

Kelly Swinney; Darryl Bornhop

Online publication date: 03 June 2010

To cite this Article Swinney, Kelly and Bornhop, Darryl(2000) 'A Review of CE Detection Methodologies', Critical Reviews in Analytical Chemistry, 30: 1, 1 — 30
To link to this Article: DOI: 10.1080/10408340091164162
URL: http://dx.doi.org/10.1080/10408340091164162

Critical Reviews in Analytical Chemistry, 30(1):1–30 (2000)

A Review of CE Detection Methodologies

Kelly Swinney and Darryl Bornhop

Department of Chemistry and Biochemistry, Texas Tech University, Box 41062, Lubbock, Texas 79409

Key Words: capillary electrophoresis, absorbance detection, (laser-induced) fluorescence, electrochemical detection, refractive index, photothermal refraction.

I. INTRODUCTION

Presented here is a comprehensive description of the four major detection modalities (absorbance, fluorescence, electrochemical, and refractive index) as well as a brief discussion of the less used detection techniques for CE. The focus of this manuscript is limited to direct, online detection techniques; therefore, detection via mass spectroscopy has not been included. The most sensitive on-line detection scheme for CE is laser-induced fluorescence detection, which is capable of single molecule detection but most often requires chemical derivatization. For CE applications needing universal detection, refractive index, conductivity detection and to some degree UV-Vis systems using the low UV (<210 nm) are suitable. In general, the detection scheme of choice is application specific and dictated by the level of sensitivity necessary (Table 1). While great strides have been made toward improved detection methodologies, if CE is to become a routine, robust and widely accepted analysis method, improvements in detection technology are still needed.

II. ABSORBANCE DETECTORS

Absorbance detectors are the most commonly used detectors for microseparations, particularly for CE. Essentially all organic molecules have appreciable absorption in the low UV (160 to 180 nm), yet access to this wavelength region is problematic due to absorbance by optics and ambient air gases. While many organics can be detected at 195 to 210 nm, in this region molar extinction coefficients are relatively low. Thus, for compounds whose structures do not include pi bonds (i.e., ions, carbohydrates, and inostol phosphates) absorption detection at wavelengths >190 nm gives relatively poor signal-to-noise ratios. Moreover, in the small i.d. capillaries (<100 μm) in which CE detection must be performed, the pathlength dependency of absorbance detection exacerbates the limitations of the technique making solutes with poor absorptivity even more difficult to analyze. So, while UV-Vis absorption techniques are applicable to an abundance of solutes, it is *not* truly universal.

A. Direct Measurements

1. Native Absorption

Because most commercial CE instruments are equipped with UV-Vis detectors, many applications have been published using native absorbance detection. For example, CE with UV detection has been used to measure the binding constants between purified calf thymus DNA and a library of designed tetrapeptides.[1] In this study, CE was utilized to separate unbound tetrapeptides from the DNA-peptide complex. Then the absorbance signal for the

1040-8347/00/$.50

TABLE 1
Limits of Detection for Different Detection Techniques in CE

Detection technique	Limit of detection (M)
Direct absorbance	10^{-5} to 10^{-6} (standard pathlength)
	10^{-6} (extended pathlength)
Indirect absorbance	10^{-5} to 10^{-6}
Photothermal refraction	10^{-7} to 10^{-8}
Direct on-column LIF	$<10^{-13}$ (chemical derivatization)
	10^{-10} to 10^{-11} (native)
Post column LIF	10^{-16} (single molecule)
Indirect LIF	10^{-5} to 10^{-7}
Potentiometric	10^{-7} to 10^{-8}
Conductivity	10^{-7} to 10^{-8}
Amperometric	10^{-7} to 10^{-8}
Refractive index	10^{-6}
Raman	10^{-6}
Radiofrequency (NMR)	10^{-3}
Radioisotope	10^{-10}
Laser-induced capillary vibration	10^{-8} (chemical derivation)
	10^{-5} (native)

unbound tetrapeptides peaks was used to create a Scatchard plot facilitating the calculation of the DNA-peptide binding constants. The K_d values reported ranged from 102 to 106 M^{-1} and correspond well with those predicted.[1] Numerous other systems have been studied by CE with conventional UV detection under native conditions. These include the separation and analysis of peptides and proteins,[2] small organic molecules,[3–5] pharmaceuticals,[6–8] and carbohydrates.[9–11] Additionally, various industrial quality control and assurance applications can be accomplished by UV-CE.

Because of Beer's Law limitations, several attempts have been made to improve absorption detection limits, without sacrificing resolution, by modification of the capillary shape or diameter in the detection zone to increase the effective pathlength.[12–15] While improvements have been realized, theoretically predicted increases in absorbance due to longer pathlengths have not been achieved. For example, the capillary modified Z-cell[16] gives only a sixfold S/N ratio because of light attenuation despite a 60 times longer pathlength.

Other flow cell "shapes" have been investigated, such as the "bubble cell".[17] Yet to date, the most promising attempt at improving detection limits by increasing the pathlength in absorbance detection has been accomplished through the use of multi-reflections and laser-based excitation. The multireflection nanoliter-scale cell (Figure 1)[14] is made directly onto the separation column by silver coating a short length of the capillary. Two windows located on opposite sides of the capillary, above and below the detection zone, are separated by a distance of 1.5 mm and serve as the entrance and exit ports for the laser illumination. Using HeNe laser illumination and this multireflection configuration, a 40-fold improvement in absorption detection limits was obtained when compared to standard on-capillary UV detection. Nonetheless, this detection cell geometry uses a few millimeters of capillary producing a relatively large probe volume (6.6 nL) resulting in a loss in separation efficiency. Furthermore, the multireflection cell functions best when a laser is used, but to be practical for CE a widely tunable or broad-band light source must be substituted for the laser; otherwise,

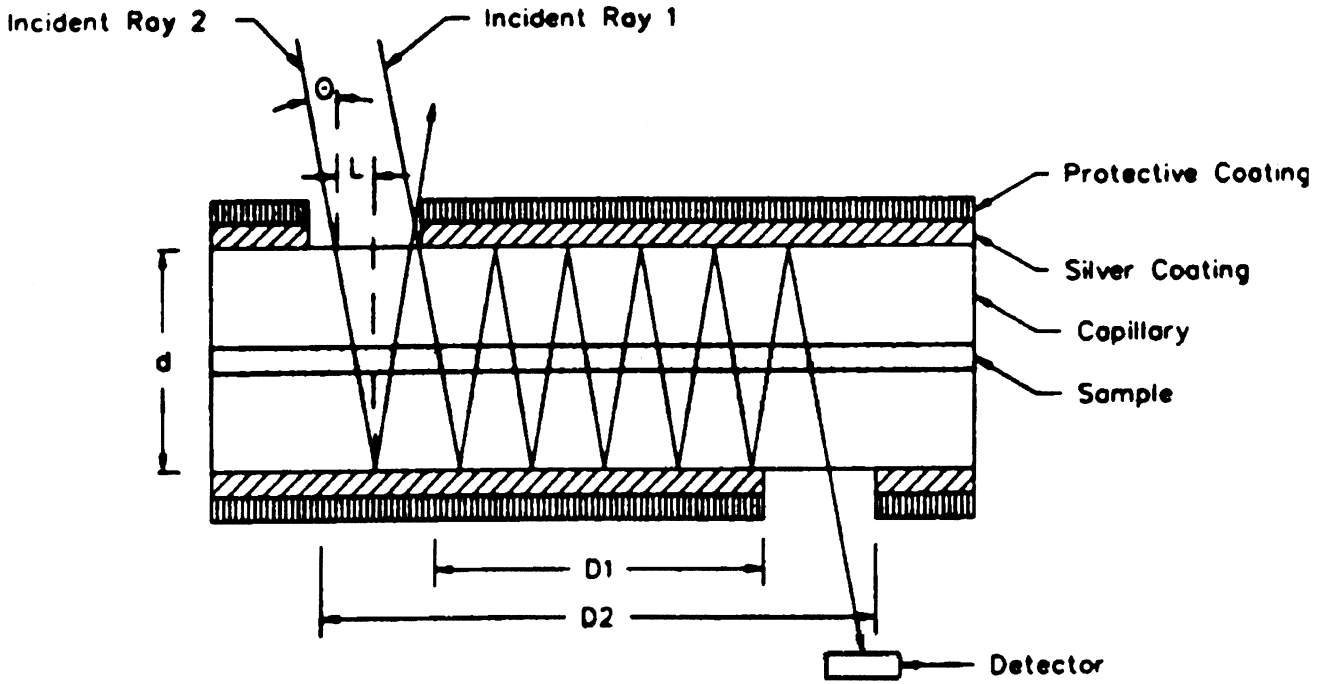

FIGURE 1. Diagram of the multireflection nanoliter scale cell.[14] The capillary is made of fused silica (75 μm i.d. × 364 μm o.d.). The silver layer was deposited by a redox reaction of $Ag(NH_3)_2$, and glucose on the section of the capillary where the polyimide coating had been removed. A protective coating of black paint was applied to the silver layer to preserve the integrity of the silver surface. The entrance and exit windows are separated by distance D_1 and D_2 (0.8 and 1.5 mm, respectively). The cell volume calculated from D_2 is 6.6 nL.

the applicability of the system would be limited to the detection of all but a few analytes. Lasers with these characteristics are still quite expensive and incoherent sources that have broad-band emission are difficult to tightly focus and because of optical constraints associated with wavelength dependency involved with refraction and reflection of light it is hard to achieve total internal reflection within the sample cell.

2. Absorption Detection Enhanced by Derivatization

When native absorption signals are weak or absent, solutes of interest are often chemically derivitized to enhance the absorption characteristics of the analytes. For example, Hu et al.[18] described a procedure for the analysis of α-difluoromethylornithine (DFMO), an anticancer agent in plasma microdialysis samples. In this procedure, a precolumn derivatization step is necessary to convert the non-UV active DFMO to N-substituted 1-cyanobenz[*f*]isoindole (CBI), which is UV active, by reacting it with naphthalene-2,3-dicarboxaldehyde-cyanide (NDA-CN) in pH 10.0 borate buffer. Using UV detection at 254 nm, the sensitivity of DFMO in plasma microdialyzate samples (L.O.D for DFMO in plasma dialzyate was reported as 5 μM) is adequate to successfully monitor the pharmacokinetics of DFMO. In another application reported recently, Novotny and coworkers[20] used the strongly UV-absorbing tag, *N*-(4-aminobenzoyl)-L-glutamic acid (ABG), for the detection of isomaltooligosaccharides under CE conditions (Figure 2). The ABG tag was coupled to the oligosaccharides by reductive amination under mild conditions. After conjugation of the tag to the analytes, isomaltooligosaccharides from a dextran hydrolyzate were separated. Minimum detectable quantities of oligosaccharides in the subpicomole range were achieved.[19]

Extended pathlength detection cells have also been used with chemical derivatization techniques to further improve detection limits using UV absorption. For example, using both a UV absorbance Z-cell and chemical derivatization, an improvement in the detection limit by a factor of 20 was achieved for the trace analysis of carbonyl compounds in rain water as reported by Bachmann and colleagues.[20] In this protocol, chemical derivatization is based on dansylhydrazine, DNSH, which reacts with carbonyl compounds to form complexes with considerably higher molar extinction coefficients.[20] As a result, limits of detection (LOD) in the range of 170 to 300 nmol/L were reached.[20] The improvement in the detection limit using a Z-cell over the results obtained by Chervet et al.[16] using no chemical derivatization is due to a difference in detection volume and separation efficiency.

Even with techniques that utilize increased pathlength cell or/and chemical derivatization, absorbance detectors are ultimately limited by Beerís Law and the constraints associated with measuring small signal changes in the presence of large backgrounds. As a result, absorption techniques have modest concentration detection limits that generally fall in the 10^{-6} *M* range.[21] For example, under essentially ideal conditions, a molar extinction coefficient of 10,000 (M/cm), a 50 μm capillary, and a typical UV-Vis capillary absorption detector with a noise level of 5×10^{-5} A.U., the solute concentration detection limit is 1×10^{-6} *M*. Eventually, a compromise between loss in separation efficiency with increased pathlength will restrict performance and thus applicability of conventional absorbance monitors for CE detection. Furthermore, direct absorption measurements are difficult, if not nearly impossible, for solutes that possess miniscule absorption coefficients thus eliminating detection of such solutes as ions or inorganic salts.

B. Indirect Measurements

An alternative way to detect molecules that do not possess appreciable absorptivities is

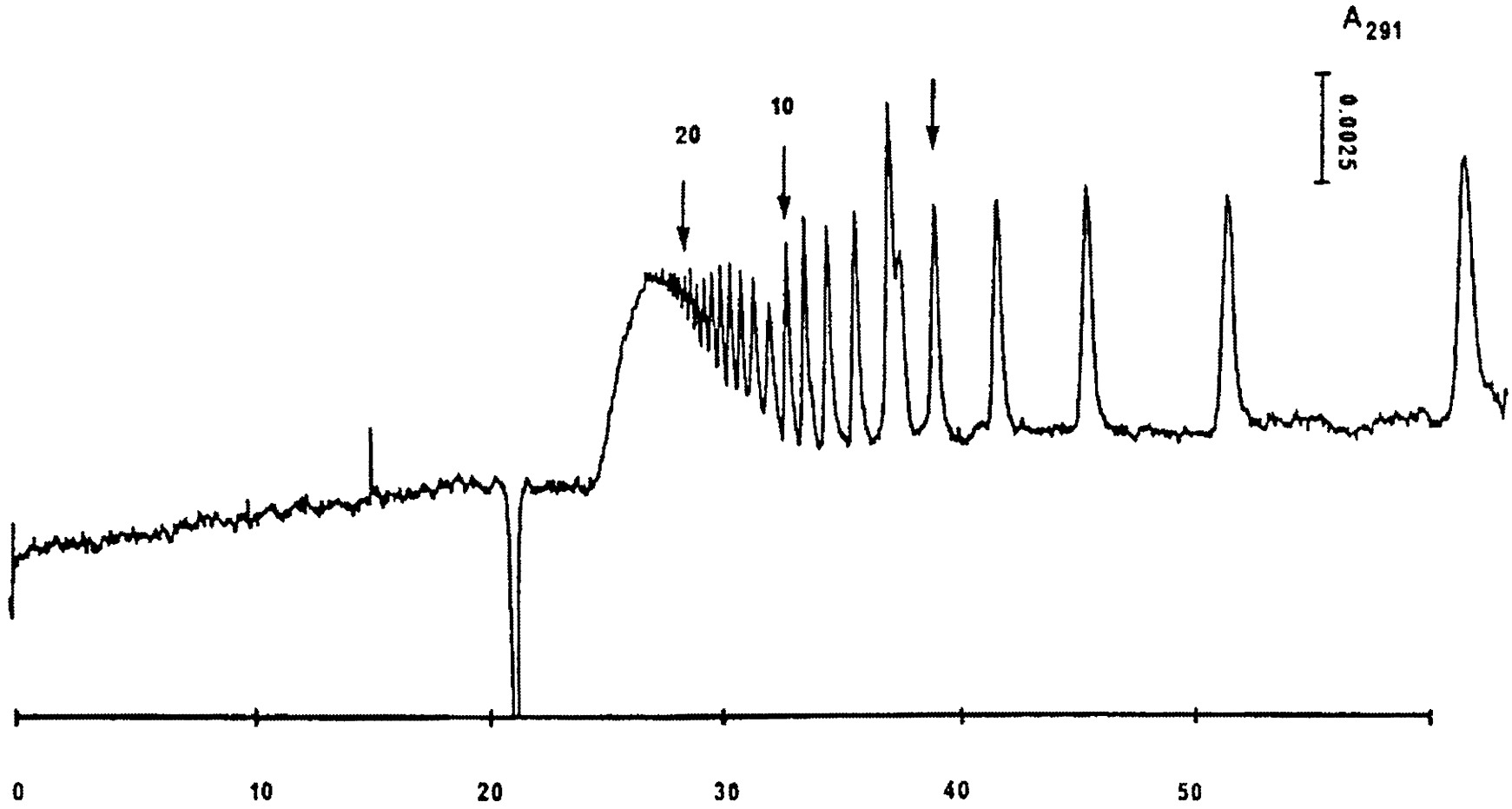

FIGURE 2. Separation of the ABG-derivatized oligosaccharides from a partially hydrolyzed dextran, in an uncoated capillary.[19] Electrophoretic conditions: applied voltage, 6 kV (40 μA); electrokinetic injection, 5 s (5 kV); 0.2 *M* sodium borate buffer (pH 10.0). 5, 10, 20 denote number of sugar units.

to use indirect methods. Indirect absorption measurements are basically vacancy techniques and in CE have primarily been used for the detection of small ions,[22–24] carbohydrates,[25] lanthanides,[26] alkyl sulfates,[27] and carboxylates.[28] In the indirect absorbance measurement,[29] as shown in Figure 3, an additive is introduced to the buffer system producing a relatively large background signal, which reduces the amount of light reaching the detector. When a solute band (having a lower absorbance than the additive) passes through the detection volume, the light throughput to the photodetector increases, providing a signal for the solute. The limits of detection for such measurements are comparable to"standard" UV-Vis absorbance and fall in the 10^{-6} to 10^{-5} *M* range.[30] However, recently Doble et al.,[31] using highly absorbing dyes such as bromocresol green and indigotetrasulfonate in order to generate large background signals, were able to detect anions at sub-μ*M* concentrations (Figure 4). According to the following equation for detection limit for a nonabsorbing analyte using indirect absorbance detection,[31]

$$C_{LOD} = \frac{N_{BL}}{R\varepsilon l} \qquad (1)$$

increasing the molar extinction coefficient (ε) of the background analyte decreases the concentration detection limit (C_{LOD}) if the background noise level (N_{BL}) is unchanged. For best performance, indirect detection requires a well-characterized displacement mechanism such as a large transfer ratio, S/A (the ratio of the number of signal generating molecules (S) displaced in the detection zone by a single analyte molecule (A)), a stable background, and careful selection of the signal generating chromophore. Indirect detection is best suited for application–specific systems in which all parameters are optimized and remain unchanged from run to run.

C. Nontraditional Absorbance Measurements

1. Photothermal Refraction

Photothermal Refraction (PTR) is a nontraditional absorbance technique that can provide impressive detection limits because the signal is shifted into a frequency region away from the background. For example, an absorbance event produces a thermal perturbation, which leads to an optical signal. PTR is pathlength insensitive, can be used directly on capillary, and therefore is a particularly attractive detection method for CE. This technique requires that two lasers to be employed, a pump

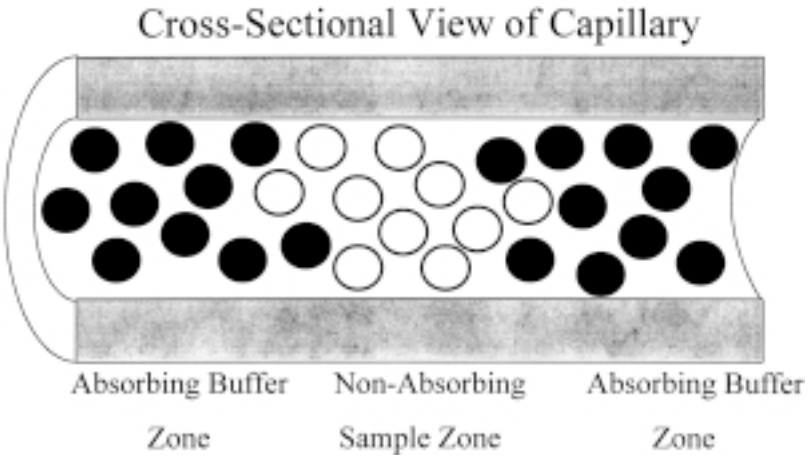

FIGURE 3. Cartoon of indirect absorption.

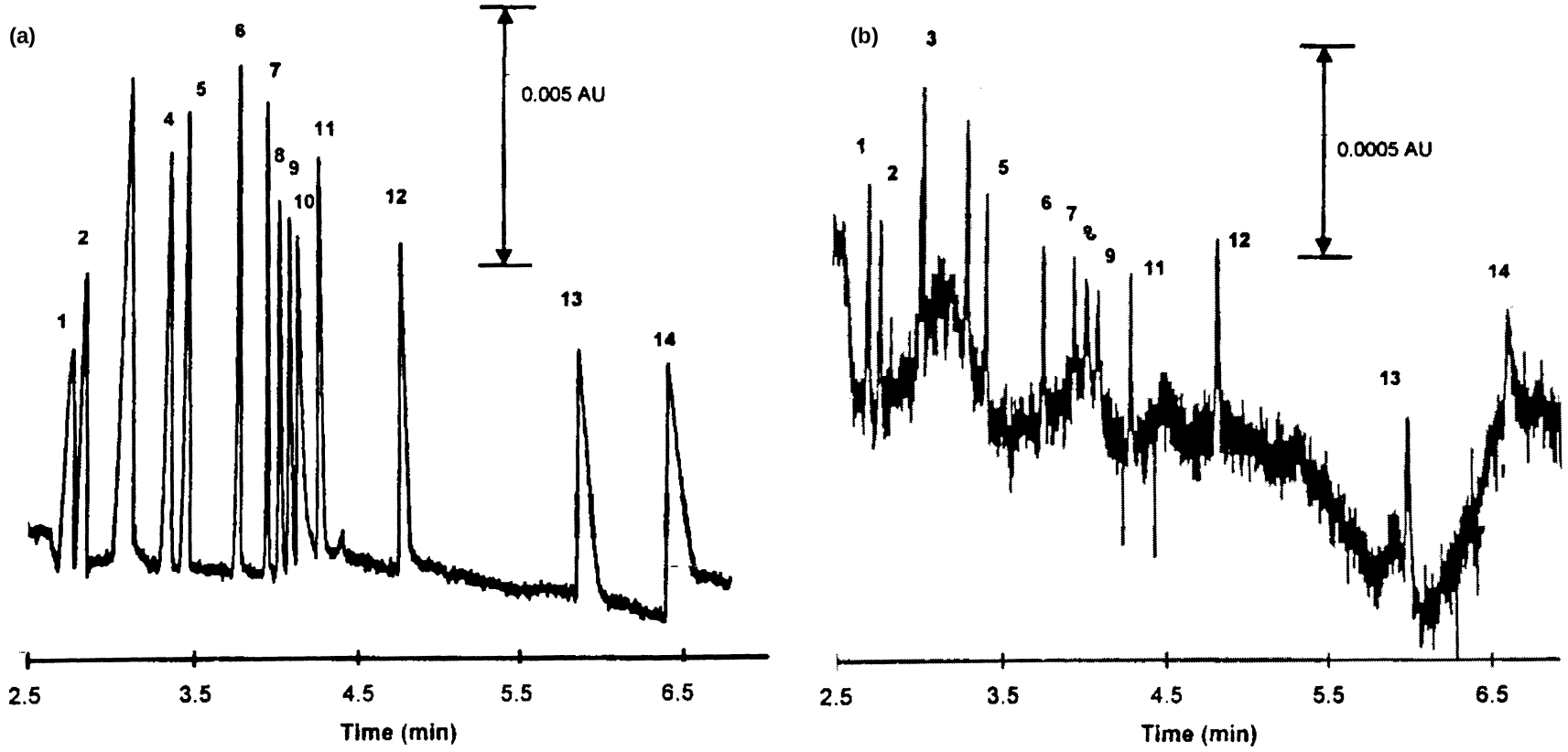

FIGURE 4. Electropherogram of 14 anions obtained from the high concentration standard (a) and near their detection limits (b) with ITS as the probe.[31] Conditions: electrolyte 0.5 m*M* ITS, 2.67 m*M* Bis-Tris, pH = 6.8, separation voltage: 30 kV, 0.6 s pressure injection at 5 in.Hg, detection wavelength 314 nm, temperature 30°C. Key: 1 = bromide (a) 200 m*M*, (b) 10 m*M*; 2 = chloride (a) 200 m*M*, (b) 10 m*M*; 3 = sulfate (a) 80 m*M*, (b) 2 m*M*; 4 = thiocyanate (a) 80 m*M*, (b) 2 m*M*; 5 = chlorate (a) 80 m*M*, (b) 2 m*M*; 6 = malonate (a) 40 m*M*, (b) 1 m*M*; 7 = tartrate (a) 40 m*M*, (b) 0.5 m*M*; 8 = bromate (a) 40 m*M*, (b) 1 m*M*; 9 = formate (a) 40 m*M*, (b) 1 m*M*; 9 = formate (a) 40 m*M*, (b) 1 m*M*; 10 = citrate (a) 30 m*M*, (b) —; 11 = succinate (a) 30 m*M*, (b) 0.8 m*M*; 12 = phthalate (a) 30 m*M*, (b) 0.8 m*M*; 13 = iodate (a) 60 m*M*, (b) 1.5 m*M*; 14 = phosphate (a) 60 m*M*, (b) 1.5 m*M*.

laser and a probe laser. As shown in Figure 5 for the cross beam thermal lens instrument, developed by Bornhop and Dovichi,[28] the pump laser and the probe laser are oriented such that they intersect within the capillary defining the detection region. When a molecule passes through the detection region, it absorbs light from the pump laser. Deactivation through a nonradiative decay pathway and the subsequent transfer of thermal energy to the surrounding buffer leads to a change in the refractive index of the buffer. This process is performed periodically (AC) by either pulsing the laser or chopping the pump beam, allowing lock-in detection and generation of the signal in the AC. As a result of periodic heating, the probe beam is refracted changing the far-field intensity, and an analytical signal is produced at an AC frequency and not in the DC regime where noise is prominent. Thermooptical absorbance sensitivity is proportional to the pump laser power and therefore, higher power lasers are useful for detecting weakly absorbing or low concentration analytes.

Thermooptical detection has been used for the detection of a variety of compounds separated by CE. Dovichi et al.[29–35] have described thermooptical absorbance systems for several different chromophore/laser combinations. For example, a 4 mW HeCd laser was chosen as the pump source for the analysis of DABSYL-derivatized amino acids.[29] For this separation, a mass limit of detection of 200 amol for DABSYL-glysine was reported.[29] Yu and Dovichi reported the detection of DABSYL-methione at a mass detection limit of 37 amol (5×10^{-8} *M* concentration detection limit) using a 130 mW-argon-ion lasers as the pump source.[30] Amino acids derivatized with phenylthiohydantoin were detected by Waldron and Dovichi using an excimer laser with reported detection limits of 9×10^{-7} *M* for glycine.[31] The detection of 19 amino acids derivatized with phenylthiohydantoin produced in the Edman degradation reaction for protein sequencing was also accomplished with thermooptical absorption techniques by Chen et al.[34] More recently, Dovichi and co-workers have applied PTR successfully to CE and CEC for the detection of five tricyclic antidepressants.[35] Others have been involved in using PTR systems for detection in CE. For exam-

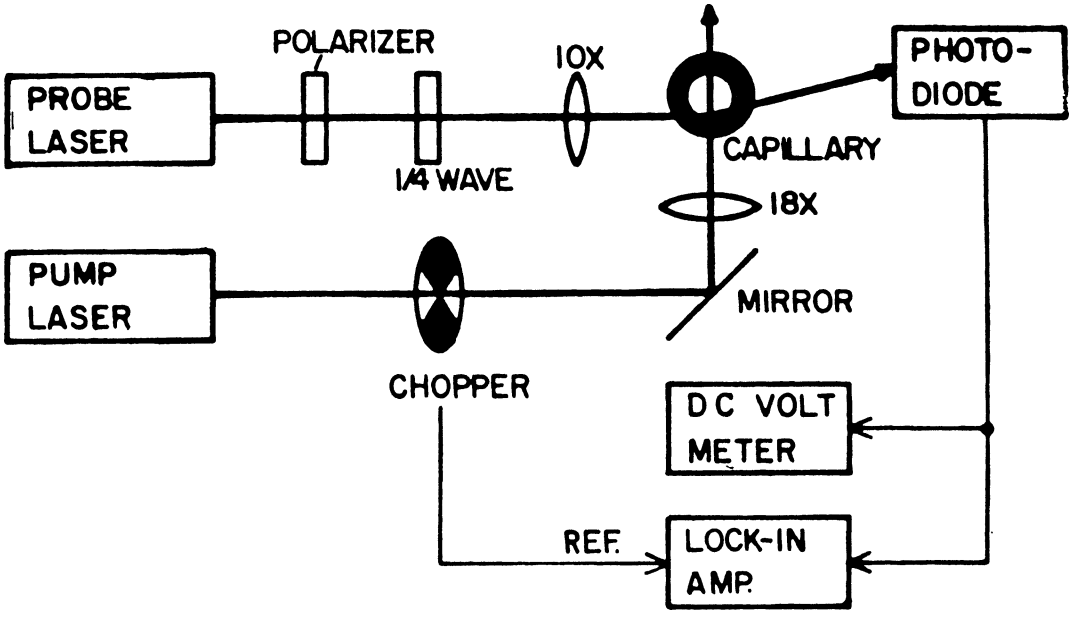

FIGURE 5. Block diagram of the cross beam thermal lens instrument developed by Bornhop and Dovichi.[28]

ple, Bruno et al.[36] have also reported the use of thermo-optical absorbance detection for CE using a frequency doubled argon-ion laser as the pump beam. Dansylated amino acids were analyzed in a 25-μm i.d. capillary[36] proving the pathlength insensitivity of thermooptical techniques. Saz et al.[37] demonstrated detection of native proteins separated by CE using PTR with 257 nm excitation and probed with a hologram-based RI detector. Detection limits of 7×10^{-9} *M* for bovine serum albumin was achieved.[37]

PTR techniques have several advantages including very small probe volumes and high sensitivity. However, tedious alignment is required for PTR to function, and the solute must have absorbance features that correspond to the wavelength of the excitation laser beam, $d\eta/dT$ for the mobile phase must be appreciable in order to produce a highly sensitive measurement, and it is relatively expensive to configure.

2. Laser-Induced Capillary Vibration Detection

Laser-induced capillary vibration is yet another detection method that can be used with CE and is considered an unconventional absorbance measurement. Laser-induced capillary vibration detection was developed by Sawada and co-workers[38–42] and is in principle a thermooptical detection technique. In the detection scheme developed by Sawada and colleques, the separation capillary is supported during the analyisis and a tension is applied to the tube by a hanging weight. A focused, intensity modulated laser source is then used to vibrate the capillary at a frequency equal to that of the modulated laser source. String-like vibration of the capillary occurs as a result of the heat generated photothermal effect induced by the laser that produces oscillations in the tension at the irradiation point. A probe beam, aligned just above the capillary at the vibration/irradiation point, is used to monitor amplitude fluctuations in the vibration that result from changes in absorption characteristics of the fluid in the detection region of the capillary. Detection of the probe beam caused by changes in the amplitude fluctuations of the capillary is monitored using a photodiode and lock-in detection and is directly related to the concentration of the absorbing solute in the detection zone. Using laser-induced capillary vibration in a detection volume of 100 pL and using an argon ion laser, Sawada et al. demonstrated it is possible to measure 6.0 fg (13 amol or 1.3×10^{-7} *M*) of sunset yellow dye, which corresponds to 1.5×10^{-5} absorbance unit.[38] This novel technique has also been used in the analysis of DABSYL derivatized amino acids[38] and under conditions optimized to reduce background signal generated from heat, 8 amol (8×10^{-8} *M*) mass detection limits were achievable.[41] More recently, Sawada and colleagues[42] successfully analyzed a series of nonderivatized amino acids at the femtomole (10^{-15} *M*) level using the vibration method and a excimer laser operated at 248 nm (Figure 6).

III. LASER INDUCED FLUORESCENCE

Laser-induced fluorescence (LIF) is the most sensitive, small-volume detection method developed to date. The limits of detection of the best CE/laser-based systems are well below 10^{-13} *M*,[43] producing mass detection limits of less than 10 molecules.[44] In fact, single molecule detection has been demonstrated in CE using LIF.[45–47] Various arrangements or approaches to LIF have been implemented, including the first on-column LIF detection system developed by Zare et al.,[48] the post column sheath flow cuvette first demonstrated by Dovichi and co-workers,[49–52] and indirect LIF.[53–55] The advantages and limitations of each technique are detailed below.

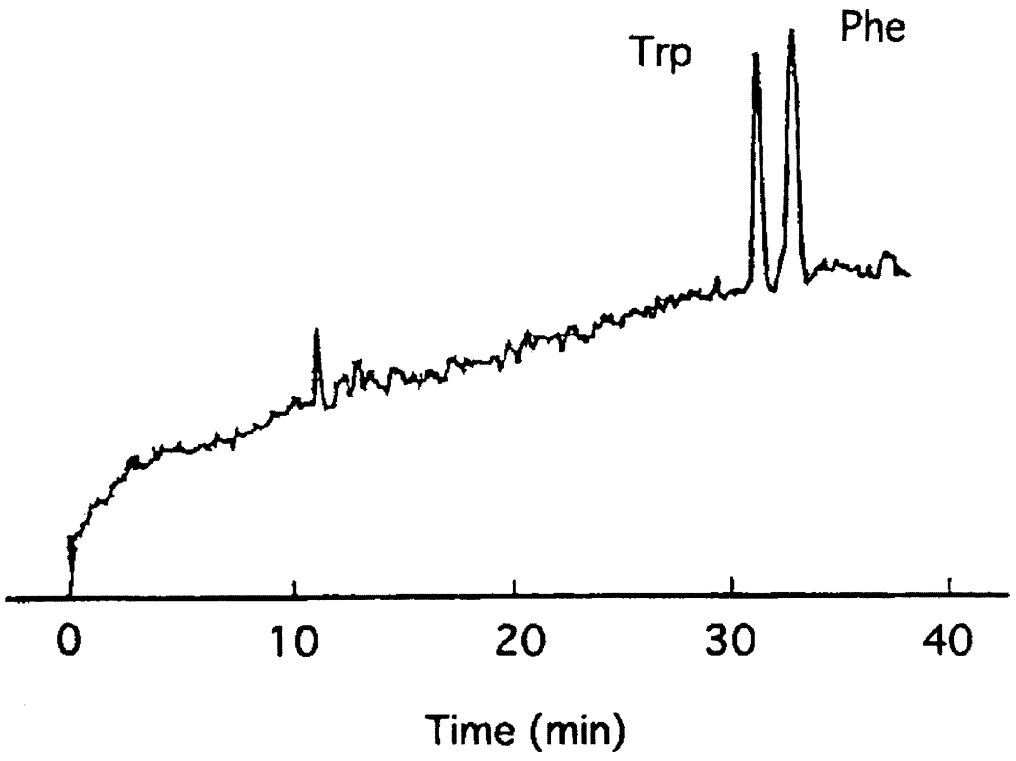

FIGURE 6. Electropherogram of nonderivatized amino acids detected by pulsed laser-induced stationary wave CVL detection.[42] Injected amounts were 0.3 pmol for tryptophan and 3.0 pmol for phenylalanine. Separation voltage of 15 kV was applied along a 75-cm-long, 20 μm i.d., 150 (m o.d. capillary.

A. Direct On-Column Detection

The first on-column LIF detection system described for CE was reported by Zare et.al. and used fiber optics to illuminate the capillary and to collect the fluorescence signal.[48] The optical configuration developed by Zare et al.[48] utilized a 325-nm HeCd laser whose output was focused into an optical fiber and used to remotely illuminate a small region of the separation capillary. Using a collection fiber, the fluorescence signal was directed into monochromator and detected with a PMT. With this optical arrangement, detection limits of approximately 200 amol (0.1 μ*M*) for dansylated amino acids was possible. Hernandez and co-workers[56,57] report zeptomole mass detection limits (10^{-13} *M* concentration detection limits) for a series of derivatized amino acids using their collinear LIF detector. In this arrangement, the angle between the exciting laser beam and the collected fluorescence is 0°, which reduces laser scattering by the walls of the capillary, leading to lower background signals and enhanced collection of the fluorescence signal. Novotny and co-workers[58] also reported the use of LIF detection for amino acids at the attomole level. Here, a modulated (mechanical chopper) HeCd laser was chosen as the excitation source and focused directly onto the capillary. The fluorescence signal (50% peak transmission) was collected at 90° with respect to the incident bean using a fiber optic whose output was focused onto a PMT in communication with a lock-in amplifier. In addition, Novotny et al.[58] used precolumn derivatization of the analytes with 3-(4-carboxybenzoyl)-2-quinolinecarboxaldehyde, an approach that has the advantages of specifically labeling the analyte of interest with a fluorophore whose excitation maximum is coincident with the wavelength

of the probe laser. Although precolumn derivatization allows molecules that do not fluoresce at available laser lines[58] to be detected via LIF, the complicated chemistry and time consuming procedures associated with derivatization make laser-induced fluorescence less attractive than universal detection methods. Swaile and Sepaniak[59] were the first of demonstrate native fluorescence with on-column detection using UV excitation (frequency doubled Ar-ion laser — 257 nm). They were capable of detecting conalbumin at a detection limit of 1.4×10^{-8} *M*. Using the same type of laser, Nie et al.[60] demonstrated improved mass detection limits (30-150 zmol or 6×10^{-11} *M*) for the detection of native fluorescence for polycyclic aromatic hydrocarbons. Yeung[61] and Sweedler[62] both have described the detection of tryptophan based on native fluorescence using a frequency doubled Kr laser (284 nm). Both groups report subnanomolar concentration detection limits (Yeung[61] — 7×10^{-10} *M*, Sweedler[62] — 2×10^{-10} *M*) with the frequency doubled Kr laser.[61,62]

The advantage of detecting native fluorescence is the elimination of precolumn derivatization steps simplifying the chemical workup and reducing the time of the total analysis. The disadvantage of using native fluorescence is that the signal is often weak and the background signal can be high, leading to poorer signal-to-noise ratios than those produced by fluorophore-tagged analytes. As a result, the sensitivity suffers. In addition, very few molecules exhibit appreciable native fluorescence, therefore the technique is limited to a relatively small class of molecules.

Post-Column Detection

Several LIF post-column detectors[46,47,49–52,63–67] have been reported, but only one method has gained wide acceptance. In all cases, the goal has been to spatially or spectrally separate the fluorescence signal from the high background signal. To date, the best performing system, which was developed by Dovichi and co-workers,[46,47,49–52,67] involves the incorporation of a sheath flow cuvette at the end of the capillary and is comprised of a 200 μm fused silica square flow chamber with 1-mm-thick windows (Figure 7). In general, sheath flow cuvettes use a flowing jacket of refractive index matching buffer to hydrodynamically focus the sample stream as it exits the capillary. The excitation laser beam is focused, using a microscope objective, into the sample stream about 30 μm below the tip of the capillary. The fluorescence signal is collected on each side the cuvette by two microscope objectives. The signal is filtered with a band pass interference filter and is imaged onto an iris (pinhole). Two photomultiplier tubes connected by a summing circuit are used to detect the fluorescence.

The sheath flow cuvette eliminates many of the problems associated with on-column detection. First, Rayleigh and Raman light scattering from the capillary is greatly reduced because at the sheath flow/sample interface there is a lack of a refractive index interface. Second, a pinhole is incorporated into the optical configuration to further minimize light scattering and reduce broad-band luminescence background from the capillary assuring that only the fluorescence emission from the sample stream is detected. Third, sheath flow cuvette is a hydrodynamic focusing technique which limits post column band broadening and allows for high-efficiency separations (1×10^6 theoretical plates). The sum of the advantages provided by the sheath flow cuvette and LIF has led to single molecule detection[46,47,67] and the ability to discern the individual behavior and activity alkaline phosphatase enzymes[46,47] (Figure 8).

C. Indirect Fluorescence Detection

Indirect fluorescence detection using LIF was first reported by Yeung and co-workers.[53,54] The concept of indirect fluorescence measurements is essentially the same as indirect absorbance measurements, except the

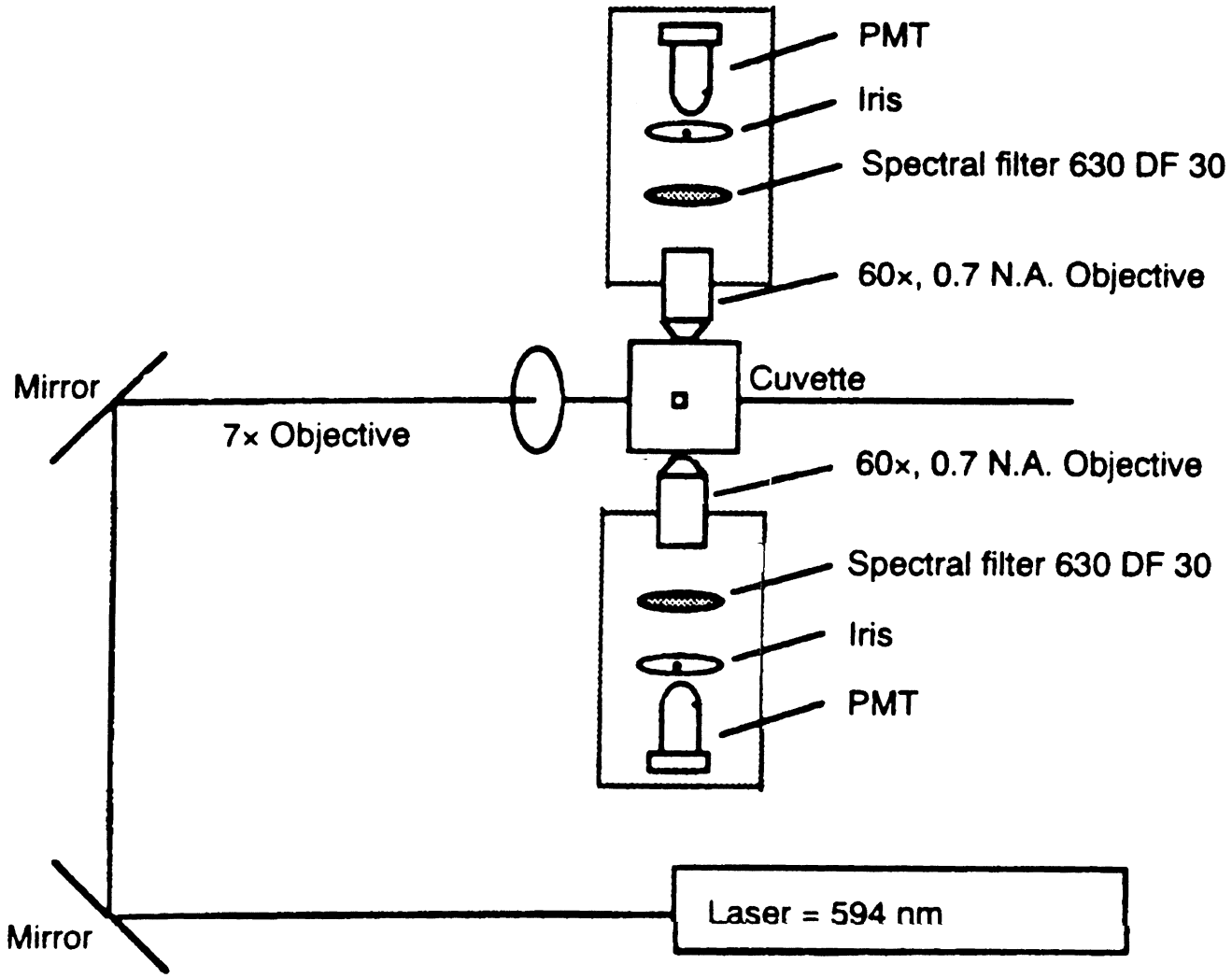

FIGURE 7. Block diagram of LIF using a sheath flow cuvette (From Chen, D. Y., Adelhelm, K., Cheng, X. L., and Dovichi, N. J. *Analyst.* **1994,** 119, 349.)

background (buffer) fluoresces instead of absorbing (Figure 9). The limits of detection for indirect fluorescence techniques generally fall in the 10^{-6} to 10^{-5} *M* range. Using the 325 nm line of a 8-mW HeCd laser for excitation and a capillary mounted at Brewster's angle to minimize the amount of stray light entering a PMT fitted with a spatial filter and a 405-nm interference filter, Kuhr and Yeung reported detection limits as low as 10^{-7} *M* for the separation of amino acids.[53] In recent months, Shamsi et al.[55] demonstrated that riboflavin-5′-phosphate (FMN) can be used as an indirect laser-induced fluorescence detection reagent for the analysis of inorganic ions and organic acids using CE (Figure 10). FMN is advantageous because it has an excitation maximum is coincident with the 488-nm line of an argon ion laser and its quantum efficiency is unaffected by pH unlike the commonly used indirect fluorescence reagent, fluorescein. Shamsi et al.[55] showed using FMN that detection limits in the range of 10 to 20 μmol/L were possible for the separation of 21 inorganic ions and organic acids. However, compared with direct LIF, poor limits of detection for indirect fluorescence measurements are the result of the noisy fluorescence background, primarily caused by laser intensity instability (flicker noise). In addition, low fluores-

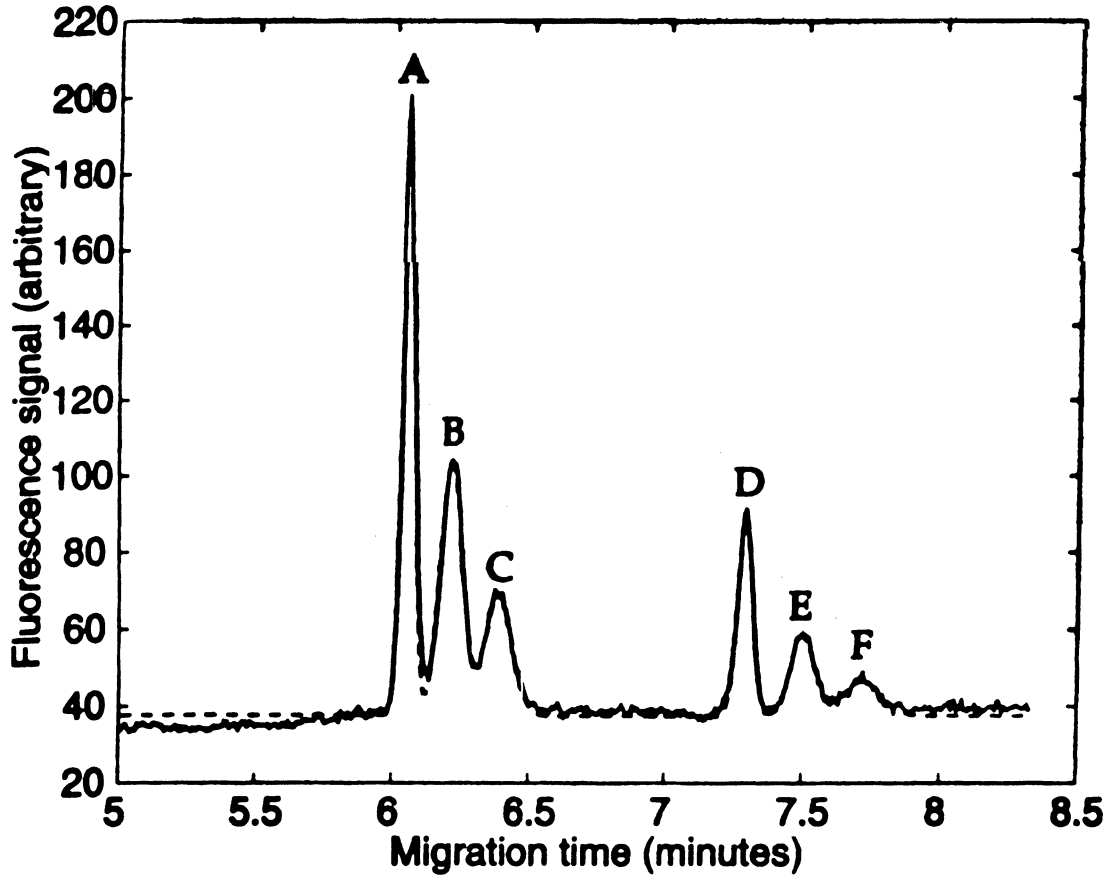

FIGURE 8. Electropherogram of alkaline phoshatase thermodynamic analysis using a sheath flow cuvette and LIF[46,47] olution of 4.6×10^{-16} *M* alkaline phosphatase in 100 m*M* borate (pH 9.5) containing 1 m*M* AttoPhos was injected onto the capillary. Sample was incubated for three 15-min periods at 16, 24, and 30°C, interrupted by brief periods of high voltage. Following the 3rd incubation, the capillary contents were electrokinetically swept through the detector. A set of three peaks is shown.

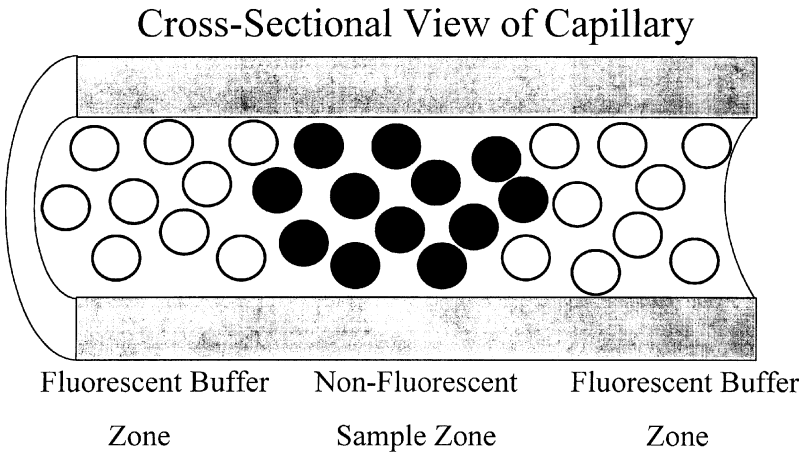

FIGURE 9. Cartoon of indirect fluorescence.

cent additive concentrations are required since excitation by laser light induces a bright fluorescence blank that can potentially saturate the PMT. Because of these low additive concentrations, the ionic strength of the electrolyte solution (buffer) is low. Low ionic strength buffers are problematic in CE because peak asymmetry often occurs at the upper end of the linear dynamic range.[21] As a result of the various limitations encountered with indirect fluorescence detection, it is not often employed in CE.

IV. ELECTROCHEMICAL DETECTION

Electrochemical detection for CE can be divided into three main categories: potentiometric, conductimetric, and amperometric. In general, conductivity and potentiometric detectors provide a bulk property response with good sensitivity. Amperometric detection, on the other hand, is selective and can be "tuned" to the analyte of interest. While some successes have been realized, implementing electrochemical detection with CE can be extremely difficult and tedious because sensor preparation can involve complicated fabrication and handling procedures, and accurate spatial alignment of the electrode within the capillary is required.

A. Potentiometric Detection

The first report of potentiometric detection in CE was by Haber and Simon in 1990.[68,69] In general, potentiometric detectors are based on classical ion-selective microelectrodes and have the ability to detect extremely small quantities of inorganic and organic ions in small probe volumes (~0.5×10^{-15} L).[21] The signal is produced when the ion of interest is transferred from the flowing sample stream into a lipophilic membrane phase of the detector. The presence of the analyte generates a change in the potential difference between the internal filling solution of the sensor and the sample stream. The potential difference is a measure of the ion's activity given by the Nernst equation and is directly related to the ion concentration. The potentiometric response is generally fast enough to prevent peak shape distortion, and therefore quantitative information about analyte concentration is possible. Yet, the disadvantages of potentiometric microsensors include tedious sensor preparation and handling procedures (i.e., preparation of the ion-selective

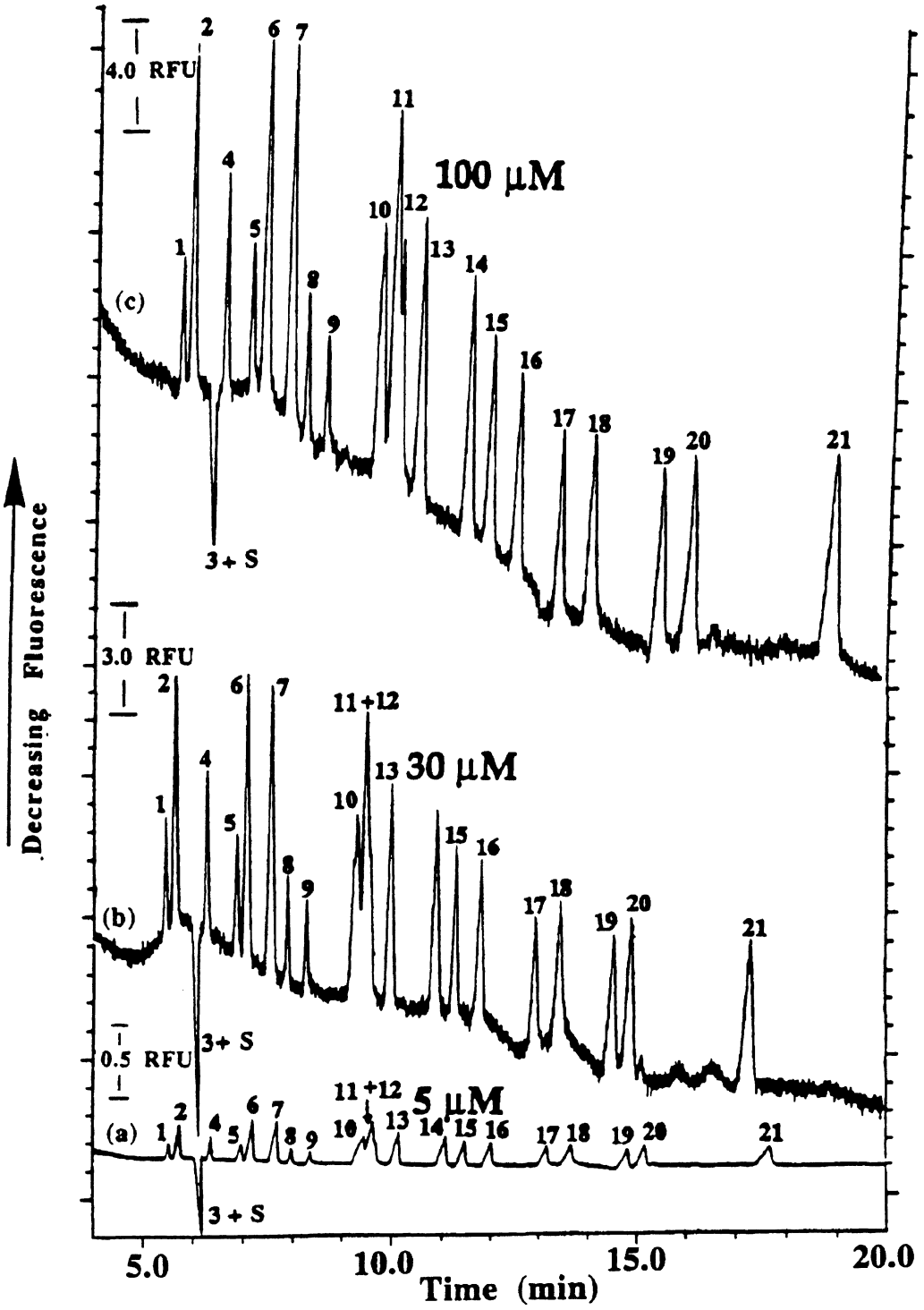

FIGURE 10. Effect of FMN concentration on separation, sensitivity, and baseline stability of a mixture of 21 inorganic anions and organic acids.[55] Electrolyte composed of 5, 30, 100 µ*M* FMN in a 100-m*M* H_3BO_3, 2-m*M* DETA, pH 7.8, buffer; pressure injection for 4 s; voltage of –15 kV applied for separation. Current varied from 6.5 to 9.0 µA. Peak identification: (1) bromide, (2) chloride, (3) nitrite, (4) nitrate, (5) chromate, (6) sulfate, (7) oxalate, (8) molybdate, (9) tungstate, (10) malonate, (11) fluoride, (12) fumarate, (13) formate, (14) succinate, (15) malate, (16) citrate, (17) tartarate, (18) phosphate, (19) hypophosphate, (20) phthalate, (21) carbonate. RFU, relative fluorescence units.

membrane phase of the microelectrode) and difficult micromanipulations necessary for alignment.[21] Another drawback of potentiometric detection is limited sensor lifetime, under normal CE conditions is approximately 2 to 3 days. Also, recalibration of the sensor is recommended every 12 h due changes in emf response of the electrode.[21]

The selectivity and response of a potentiometric sensor is directly related to the CE electrolyte solution and the internal filling solution of the electrode. For the detection of cations, the running electrolyte solution normally consists of 20 m*M* $MgAc_2$/HCl at a pH equal to 5.14 and an internal filling solution of 20 m*M* $MgCl_2$.[68] Under such conditions, the concentration detection limits for the analysis of alkali and alkaline earth cations in a 25-μm i.d. capillary were reported by Haber and Simon[68] to be less than 10^{-8} *M*. Modifying the running electrolyte solution to be 20 m*M* $MgAc_2$ at a pH equal to 7.8, the detection of amphetamines at similar detection limits ($<10^{-8}$ *M*) are possible.[69] Anions can be detected using potentiometric techniques with an electrolyte solution that is anion selective. For example, an electrolyte solution consisting of 20 m*M* Tris-formate at pH 7 allows for the detection of inorganic anions such as perchlorate at a detection limit of 5×10^{-8} *M*[70] (Figure 11).

B. Conductivity Detection

Typically, ion analysis in CE has been accomplished with conductivity detection because ions have essentially no absorption and fluorescence features. In general, conductivity detectors consist of two electrodes, in contact with the electrolyte solution, across which an electrical potential has been applied. When an analyte passes through the electrode gap, the conductivity between the electrodes changes by an quantity directly related to the concentration of the ionic analyte. Conductivity detection limits range between 10^{-6} and 10^{-7} *M* for samples introduced by electrokinetic injection.[21,71–74] For example, Rosso and Bossle[75] applied conductivity detection and CE to the screening of nerve agent degradation products in environmental samples (Figure 12). More specificly, methylphosphonic acid (MPA) degradation products of V and G nerve agents, such as Et methylphosponic acid (EMPA), iso-Pr methylphosphonic acid (PMPA), and pinacolyl methyphosphonic acid (IMPA), were analyzed for in surface water, groundwater, and soil extracts. Detection limits of 6 μg/mL were achieved using an electrolyte solution consisting of 30 m*M* 1-histidine, 30 m*M* 2-(*N*-morpholino)ethanesulfonic acid, 0.7 m*M* tetradecyltrimethylammonium hydroxide, and 0.03 wt. % Triton X-100.[75]

An improvement in the detection limits to 10^{-7} to 10^{-8} *M* can be achieved by replacing standard conductivity detection with suppression conductivity detection for the analysis of anions.[76–78] In suppression conductivity, the buffer counterion is replaced by ionic exchange or electrodialysis producing a weakly dissociated acid (anion analysis) or base (cation analysis). Consequently, the total electrolyte (buffer) conductance is lowered and the conductivity difference between the sample ion and ìbackgroundî is enhanced. Suppression conductivity, however, is problematic for cations because of its low pH buffer requirement because low pH buffers result in weak EOFs, which prevent efficient transport through the suppressor membrane to the detector. Furthermore, suppression conductivity detection is a postcolumn detection technique that induces extra column band broadening and limits separation efficiency by producing dispersion at the membrane/detector connection.[21]

C. Amperometric Detection

Amperometric CE detection was first reported as a detection technique for CE by Wallingford and Ewing in 1987 for the quan-

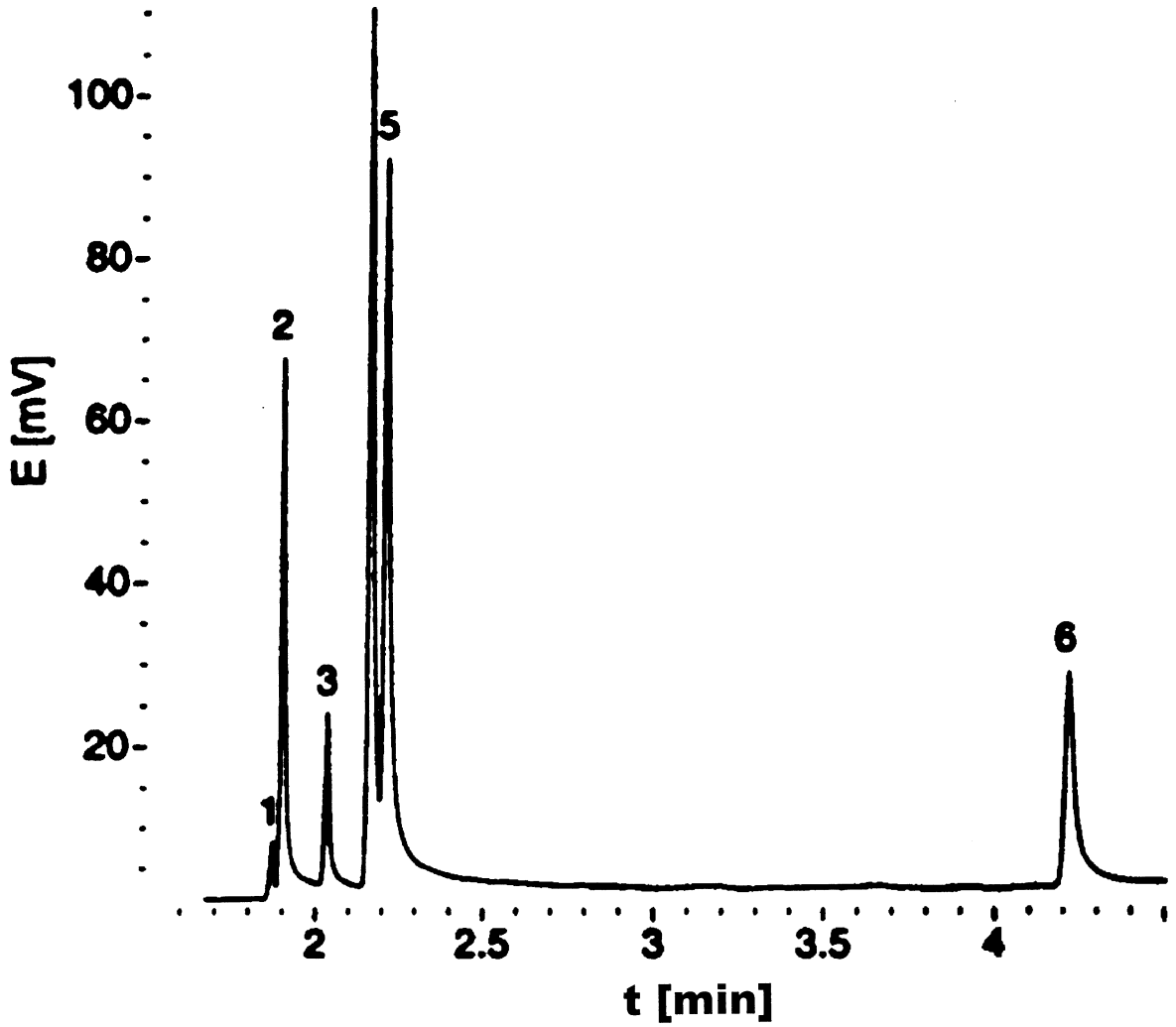

FIGURE 11. CZE-ISME analysis of Na^+ salts of (1) Br^-, (2) I^-, (3) NO_3^-, (4) ClO_4^-, (5) SCN^-, and (6) salicylate, each 10^{-4} *M* in background buffer. Buffer: 20 m*M* Tris-formate, pH 7.0; separation voltage: 25 kV; electrokinetic injection: 3 kV for 3 s. Polybrene coated capillary.[70]

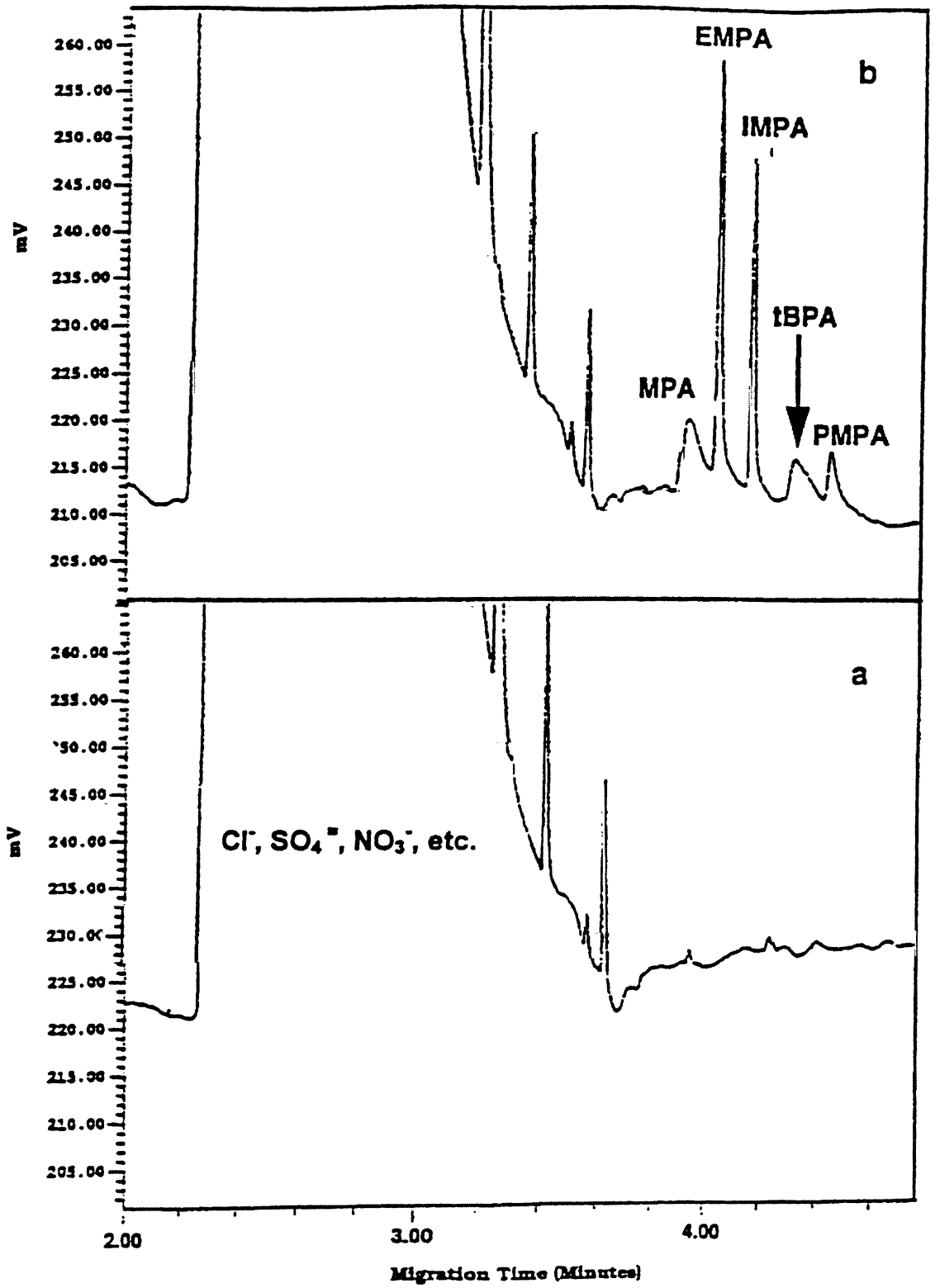

FIGURE 12. Electropherograms of Baltimore Harbor water blank (a) and Baltimore Harbor water spiked at the 10 µg/mL concentration level (b).[75] Separation conditions: buffer = m*M* MES, 0.7 m*M* TTAOH (pH 6.5), 0.03 weight % Triton X-100; separation volatage = –25 V; capillary temperature = 35°C; pressure injection at 25 mbar for 12 s.

titation of catechol and catecholamines.[79–83] Amperometric detection is based on electron transfer to or from the analyte of interest at an electrode surface that is under the influence of an applied DC voltage. The result of electron transfer is a redox reaction at the electrode that produces a current that is directly related to the analyte concentration. For example, Olsson et al.[84] demonstrated that CE with amperometric detection could be used to analyze ascorbic acid in a single protoplast (a plant cell without a cell wall) (Figure 13). Using a carbon fiber disk electrode, detection limits of 22 n*M* were determined for the analysis of ascorbic acid standards.[84] However, after the analysis of single protoplasts, 5 μM detection limits were reported for the analysis of the same solute.[84]

The major drawback of amperometric techniques is strong absorption of the intermediate reaction products of the analyte to the electrode surface (carbon electrodes) subsequently reducing the activity (electron transfer) of the electrode and interfering with detection. This problem can be reduced by using pulsed amperometric detection (PAD) which utilizes a three-step potential waveform (step 1 — detection, step 2 — anodical cleaning of electrode surface, step 3 — reactivation).[85] PAD was first reported as a detection technique in CE for the detection of carbohydrates. Using gold electrodes in an end-column configuration and PAD, mass limits of detection ranging from 0.28 fmol (10^{-6} *M*) for inositol to 1.21 fmol (10^{-6} *M*) for maltose were achieved.[86,87]

Recently, Zare and co-workers[88] have shown that intermediate absorption to the electrode does not occur when the copper electrodes are used in place of carbon electrodes eliminating the need to clean the electrode even under standard amperometric conditions (no pulsing). Therefore, a single waveform can be applied to the electrode. Using the copper electrode, 50 fmol mass LOD are possible for carbohydrates.[88] More recently, copper disk electrodes were employed by Lin et al.[89] to simultaneous detect ribonucleotides, ribonucleosides, and purine bases with reported mass detection limits below 10 fmol (Figure 14).

V. REFRACTIVE INDEX DETECTION

Refractive index (RI) detectors, in general, are bulk property, nondestructive sensors that are mass sensitive, and as such they are poten-

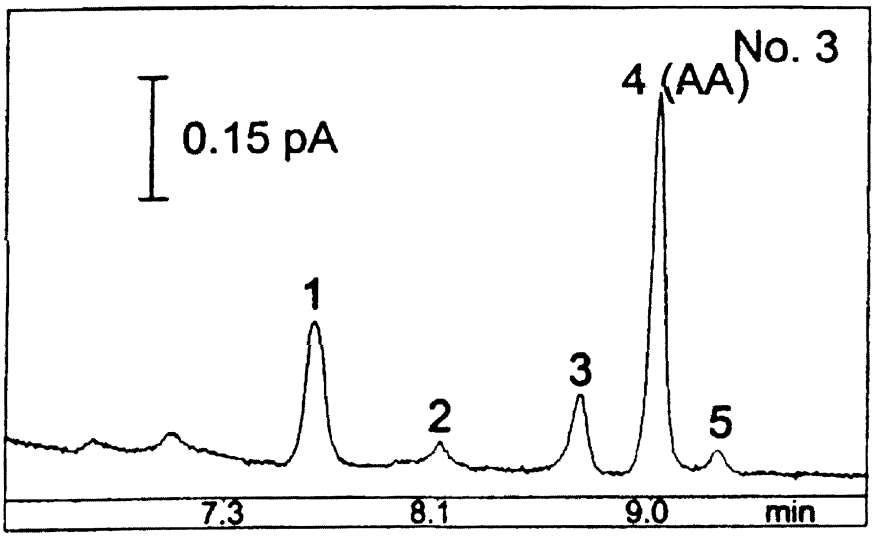

FIGURE 13. Electropherogram of a single protoplast lysed in the capillary.[84] AA, ascorbic acid. Amperometric detection at a 30-μm carbon fiber disk electrode, 1.0 V vs. Ag/AgCl; buffer: 10 m*M* phosphate, pH 7.0; capillary: 67 cm × 20 μm I.D.; separation potential: 30 kV.

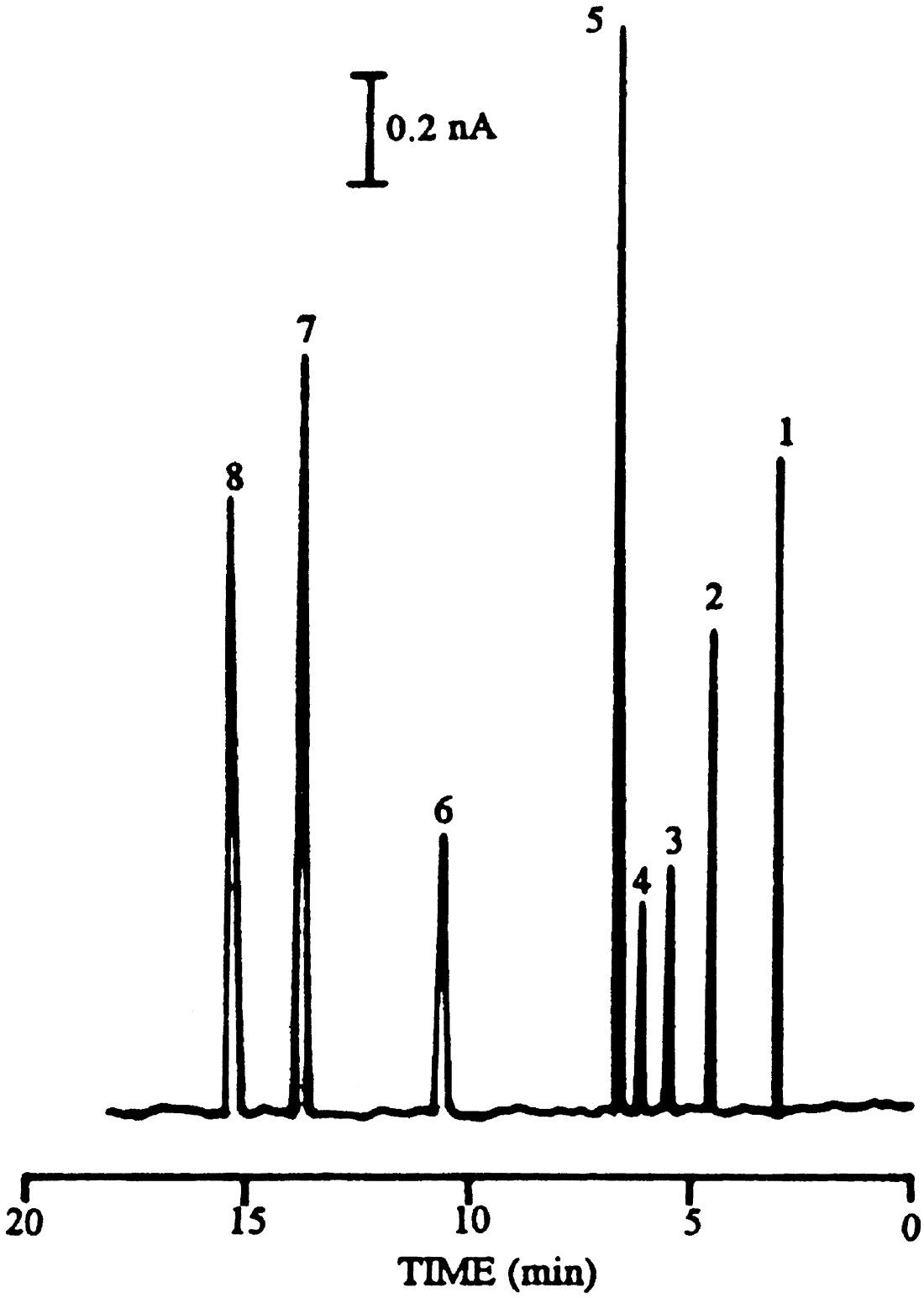

FIGURE 14. Electropherogram of the separation of ribonucleotides, ribonucleosides, and purine bases using amperometric detection and copper disk electrodes.[89] (1) 20 μM Ado; (2) 20 μM Guo; (3) 40 μM Ade; (4) 20 μM 5′-AMP; (5) 10 μM Gua; (6) 20 μM 5′-GMP; (7) 20 μM Xan; (8) 20 μM UA. Separation conditions: separation voltage, 12.5 kV; injection by electromigration, 3 s at 12.5 kV; buffer 40 m*M* NaOH; electrode potential, +0.65 V vs. SCE.

tial candidates for use as universal detection in CE. Yet implementation of RI detection schemes pose a special challenge when small volume detection is required as in CE. First, most conventional RI techniques are pathlength sensitive making detection in capillaries intractable. Second, the change in RI with temperature (dn/dT) is large (8×10^{-4} RIU/°C for water)[90] for most fluids, thus small changes in temperature result in appreciable RI signals. Even so, many attempts have been made[90–99] to miniaturize these bulk property optical detectors to nanoliter volumes.

Because of the unique optical properties of the laser (i.e., high spatial coherence and monochromaticity), they have become the 'source of choice' in the effort to construct microvolume RI detectors.[90–99] Many RI detection methods have been investigated for CE, including a concentration gradient method, which probes the on-axis optical perturbation produced by a transient solute band[97] and the use of a tapered fiber optic,[99] which probes the reduction in transmitted beam intensity due to refractive index interfacial beam intensity coupling. While powerful, these approaches to RI sensing have limitations. For example, the concentration gradient detector[97] is somewhat insensitive to thermal noise, but most suitable for detection schemes in capillary isoelectric focusing or for separation systems where postcolumn detection is acceptable.

Most state-of-the-art RI measurements involve some form of interferometry, a measurement technique that is critically dependent on the characteristics of laser light. In general, very small phase changes caused by optical path length differences, in response to the analyte, allow for high sensitivity.[100,101] The use of interferomteric techniques has produced some impressive results toward measuring RI changes in the small volumes[92,93] characteristic of CE, yet sensitivity dependency on pathlength has persisted. Bruno and co-workers[92] further developed the forward scatter, off-axis technique originally developed by Bornhop and Dovichi[91] for HPLC detection. The forward scatter technique optical configuration consists of a tightly focused laser beam, which impinges a capillary tube off axis creating an array of scattered light in the far field (forward direction). Intensity/positional changes in the forward scattered light due to changes in refractive index is detected resulting in an analytical signal. Bruno et al.[92] showed enhanced performance is possible by using a RI-matching fluid to surround the capillary tube, a flow cell assembly with active thermal control and position sensitive detection. These improvements facilitated the use of the RI detector for capillary electrophoresis for the detection of saccharose at a 2σ limit of detection of 10 μM,[92] yet the device still requires off-axis alignment and is limited by the need to remove the polymer coating from the tube to aid in index matching.

Another technique for detecting changes in **n** within capillary tubes uses a holographic grating to produce two-beam interference in a forward scatter configuration.[93] Krattiger and co-workers were able to separate and detect metal ions by CE[93] using a holographic grating, a capillary that is encapsulated in an index matching glue and a photodiode array wired to produce position sensitive detection. Manz et al.[98] recently reported the application of the holographic forward scatter RI detector for CE on a chip. The holographic technique is a significant advance toward developing a small-volume RI detector and eliminates the need for the capillary to serve as the optic, yet it is another arrangement of the forward-scattering refractive index technique with its limitations.[91–93,98] The major drawback of holographic interferometric or grazing angle forward scatter optical configurations is an inherent path length dependency, which ultimately hinders detection limits in ultra-small volumes.

Deng and Li,[96] acknowledging the difficulties with forward-scattering techniques, recently have shown that a retroreflected beam interference technique similar to MIBD[90,94,95] can be used for RI detection in capillary electrophoresis. In their scheme, a focused laser beam impinges on a bare capillary surface, caus-

ing interference of two retroreflected beams originating from the outer surface of the capillary. By observing the retroreflected interference pattern, RI measurements are possible. The main drawbacks of the retroreflected beam interference RI detector is poorer detection limits than previously reported RI detectors[90–95] and enhanced complexity of the optical train.[90,94,95]

Recently, Borhop and co-workers[90,91,94,94,102–104] introduced an alternative approach for on-column refractive index measurements based on interferometric backscatter. Using a slightly tilted, side illuminated fluid-filled capillary tube, in a backscatter configuration (Figure 15), high-contrast interference fringes are produced that move spatially in response to changes in optical pathlength allowing for refractive index detection at a level of two parts in 10^7 RIU.[94,95] The backscatter configuration exhibits essentially no pathlength sensitivity for capillaries ranging in tube size from 75 to 775 μm,[95] requires no special optical alignment, no beam-conditioning optics (lens or microscope objectives), and no modification of the polymer-coated tube. Additionally, the MIBD detection limits have been directly compared to a standard commercial UV-Vis detector performance for CE and the detection of a series of dyes with high-absorption coefficients.[103] The functional detection limits of the MIBD-RI detector were shown to be a factor of 1.6 to 2.5 times better than those reported for the standard UV-Vis absorption detector for a 100-μm capillary.[103] Due to the path length sensitivity of absorption detectors (Beer's Law), after reducing the capillary diameter to less 50-μm i.d., it was reported that the detection limit for MIBD is expected be at least five times better than for the standard UV detector. Moreover, MIBD is capable of picogram mass detection limits in nanoliter volumes with minimal passive thermal control for the detection of carbohydrates [103], organic dyes (Figure 16),[103] caffeine[102] and cations.[104] MIBD has also been shown to be a successful detection methodology for CE in the planar format (chip-scale) (Figure 17). Ignoring dilution from the separation process, and even with a extremely wide elution event (significant band broadening), the 3σ detection limit is about 875 μmolar or about an order of magnitude better than previously reported results using the holographic forward scatter technique for RI detection on a chip.[98]

Refractive index detectors are advantageous because they are universal in nature. As a result, they possess wide applicability. Furthermore, no chemical derivatization steps are necessary for detection as in LIF, thus no pre-column workup is involved. However, be-

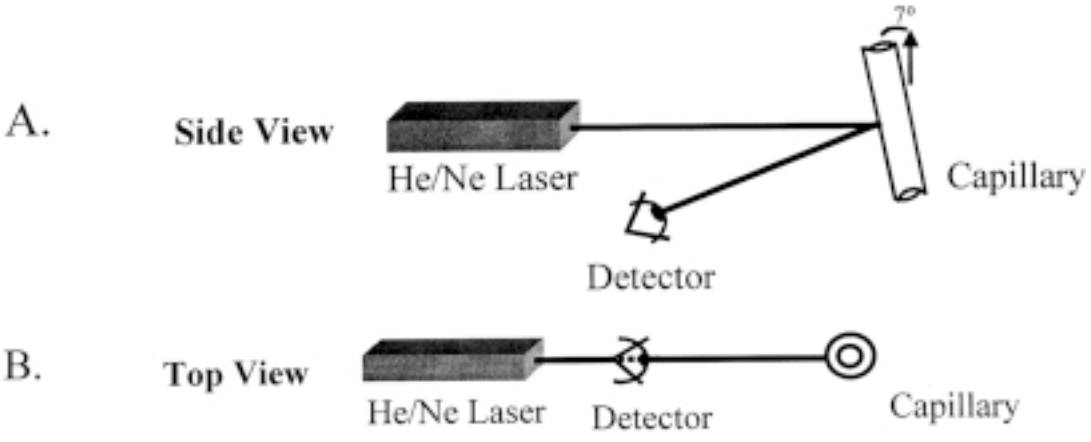

FIGURE 15. Block diagram of the microinterferometric backscatter detector (MIBD).[90,94–95,102–104] (A) Top view. (B) Side view.

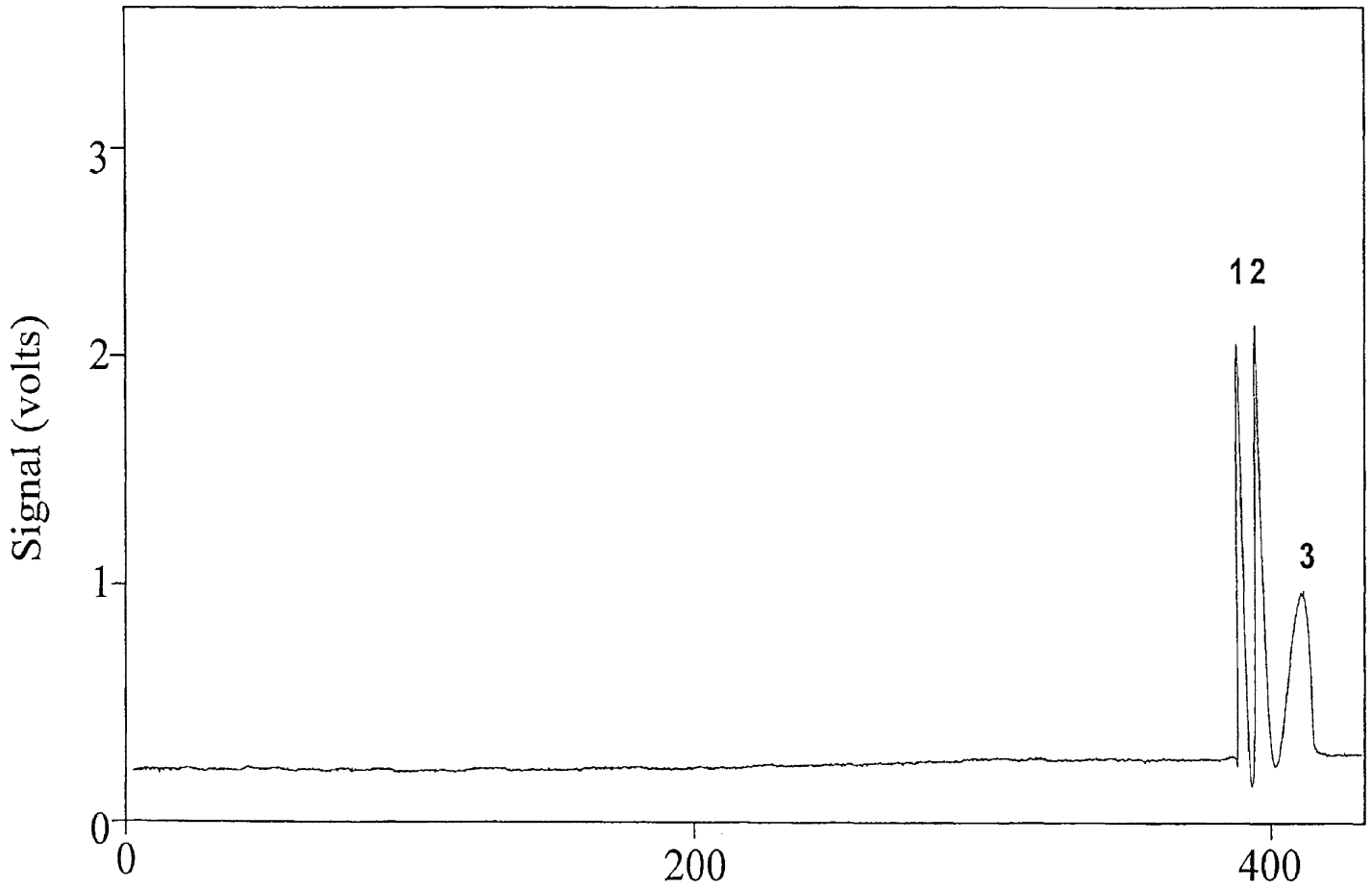

FIGURE 16. Electropherogram for a series of organic dyes detected using MIBD (RI) detection.[103] Peaks: 1 = 30 μM Bromothymol Blue, 2 = 60 μM Thymol Blue, 3 = 30 μM Bromocresol Green.

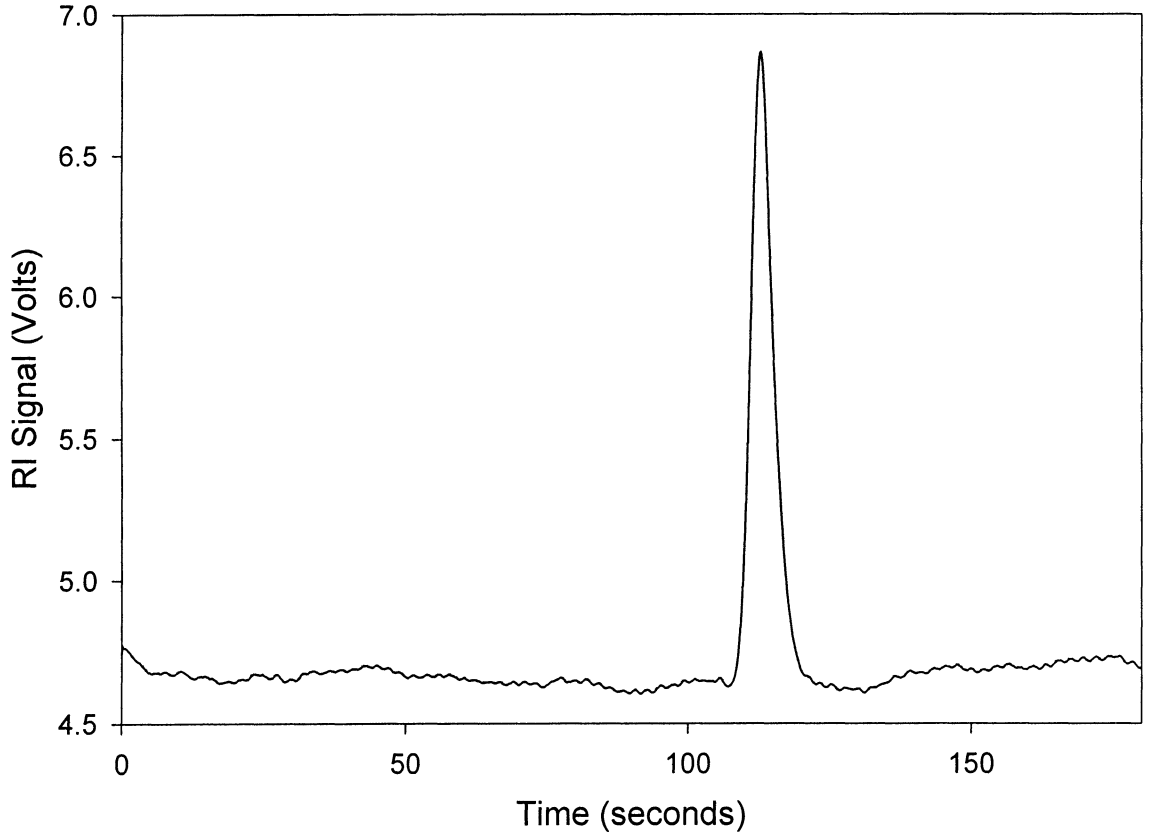

FIGURE 17. Chip-scale analysis: electropherogram of a single solute (33 m*M* sucrose) detected using MIBD in a planar format with a 50-μm radius etched channel. The sample was injected for 3 s at 3 kV and electrokinetically eluted using 5 kV. A buffer consisting of 30 m*M* Boric acid and 100 m*M* TRIS was used.

cause of their universal nature, RI detectors are not very specific. Hence, in applications where specificity is required RI detectors must be coupled with or replaced by other detection methods (LIF, absorbance, or amperometric detection).

VI. RAMAN-BASED DETECTORS

Raman-based detection is useful for obtaining qualitative information (i.e., structural details) about the analytes being separated. However, in order for solutes to be detected, they must be Raman active (polarizable). In general, the signal is obtained by monitoring changes in intensity and frequencies of scattered light induced by solutes passing through the detection zone. In the on-line Raman spectroscopy/CE system developed by Chen and Morris,[105] a 40-mW HeCd laser is used for excitation and is focused by a microscope objective onto the capillary. The scattering signal is collected by an array of 10- to 200-μm quartz fiber optics that directs the scattered light into a monochromator with PMT detection. Using this optical configuration, detection limits of 2.5×10^{-6} *M* were reported for methyl red and methyl orange under CE conditions. Such concentration detection limits compare favorably with UV-Vis detection while providing structural information. More recently, Walker and Morris[106] have reported the use of a fiber optic raman sensor using a 2-W, 532-nm, Nd/YAG laser to obtain online normal Raman spectra of AMP, CMP, GMP, and UMP separated by capillary isotachophoresis. In addition, Walker and Morris[107] have

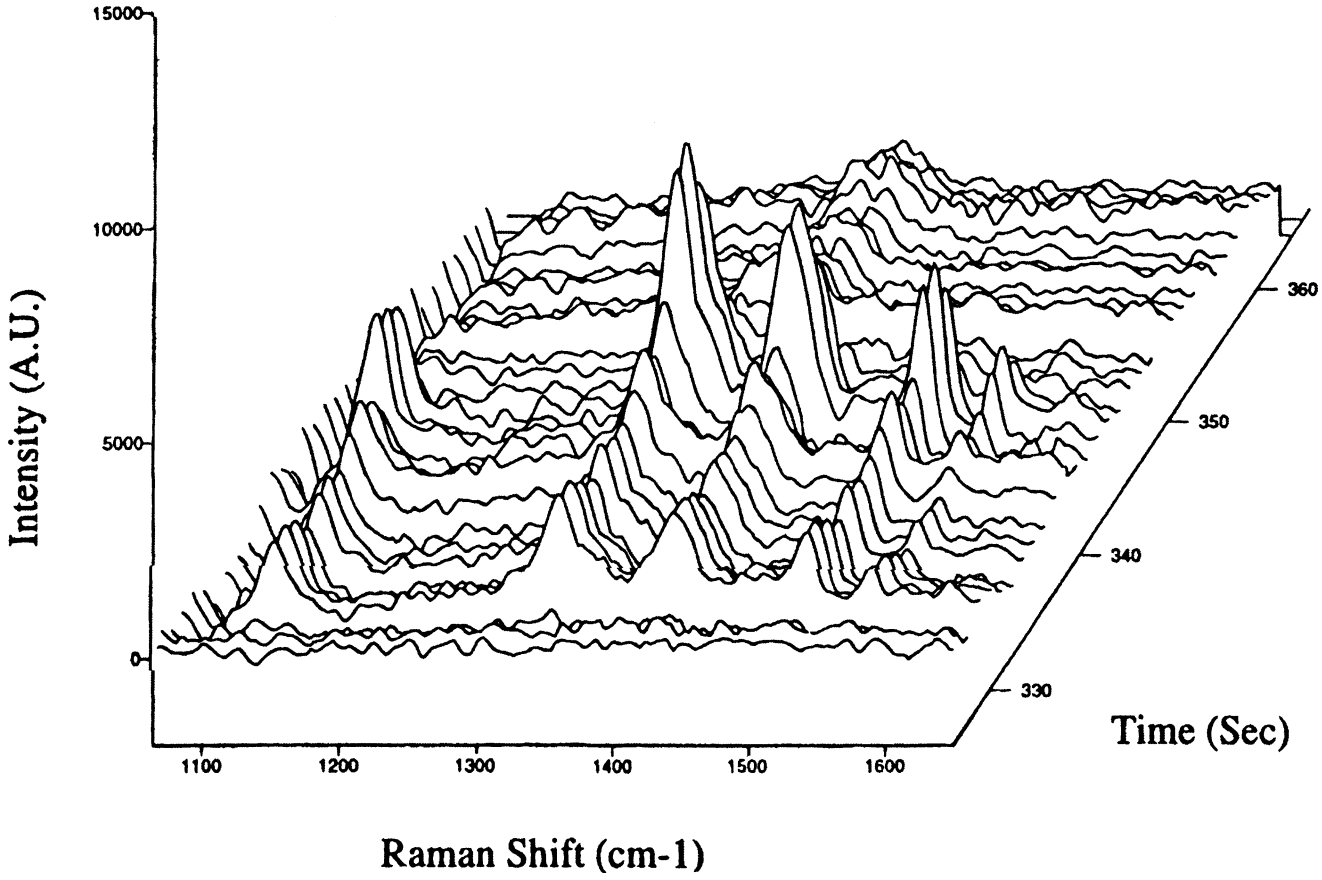

FIGURE 18. On-capillary Raman spectra of 5×10^{-5} *M* ATP, ADP, AMP preconcentrated by isotachophoresis: injection time 30 s at –4.2 kV; 400 mW 532 nm excitation; 1 s integration; resolution 16 cm^{-1}. The spectra have been ratioed to the background electrolyte spectrum and subjected to seven point Savitsky-Golay quadratic smooth.[107]

used the Raman detector for the online capillary isotachophoresis analysis of ATP, ADP, and AMP in phosphate buffers (Figure 18). Limits of detection are reported at 5×10^{-6} *M* for the ribonucleotides.[107]

VII. UNCONVENTIONAL CE DETECTION METHODS

Numerous other detection methods have been used with CE. For example, online NMR detection was first shown to work with CE by Wu et al.[108,109] and has been used for the analysis of peptides.[110] In general, NMR probes consist of 1-mm-long solenoidal microcoils that are fabricated from 50-μm-diameter wire wrapped around the outside of the separation capillary to create nanoliter volume detection cells.[111] The capillary/microcoil assembly is then orientated at a 54.7° angle with respect to the external magnetic field in order to obtain optimal sensitivity.[104] Using this arrangement, Sweedler and co-workers[111] have shown that NMR detection can be used in stop-flow CE analysis and achieves nanogram sensitivity for arginine and triethylamine (TEA), 7 ng (330 pmol; 31 m*M*), and 9 ng (88 pmol; 11 m*M*), respectively (Figure 19). Although other methods are more sensitive (i.e., LIF), using NMR detection structural information can be obtained.

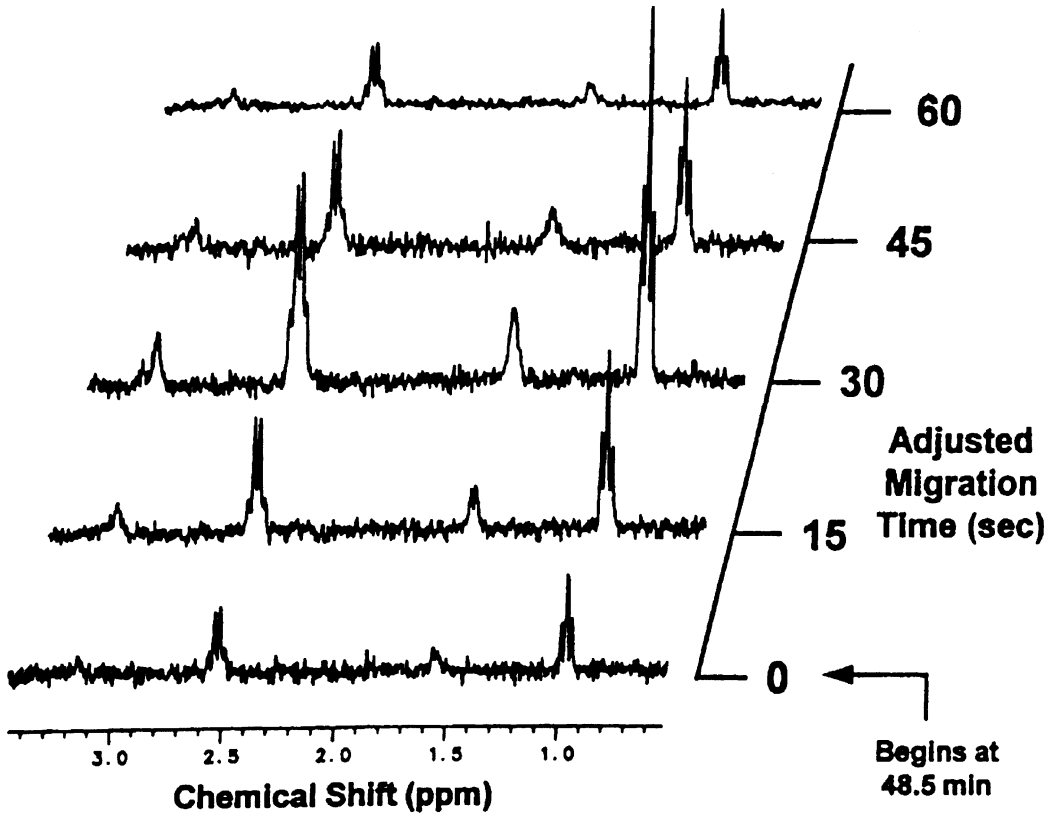

FIGURE 19. Periodic stopped-flow NMR spectra of the stacking event for a mixture of both Arg and TEA (both initially 50 m*M*).[111] A volume of 290 nL is injected gravimetrically (height of 20 cm for 22 s). Arg appears at 3.1 and 1.5 ppm, and TEA is observed at 2.5 and 1.0 ppm. NMR acquisition conditions: 40 scans in 1 min., spectral width ±2000 Hz, 8192 complex points, line broadening of 1.0 Hz. TEA and Arg are spectrally distinct. The first 48.5 min. of migration time has been omitted clarity.

Another example of less widely used CE detection is radioisotope detection. Radioisotope detection is an extremely sensitive and highly selective technique that is based on scintillation counting of the CE eluent. Pentoney et al.[112,113] first described the online semiconductor radioisotope detector that is positioned at the end of the capillary. Using this detector, ^{32}P-labeled solutes such as adenosine triphosphate (ATP) and guanosine triphosphate (GTP) can be detected at a limit of 1×10^{-10} *M*.[112] Pentoney et al.[113] also have described an on-column radioisotope detector for CE. Sensitivity of the on-column detector[113] is similar (10^{-10} *M*) to the postcolumn detector[112,113] for the analysis of radiolabeled ATP, and cytidine-5′-triphosphate (CTP). Although both radioisotope detectors are extremely sensitive, applications are limited to beta and gamma emitters. Furthermore, radioactive waste is produced, which is dangerous to handle.

VIII. SUMMARY

In conclusion, there are a number or different detection methods that can be used with CE. In general, detector selection is dependent on the proprieties of the solutes being analyzed and the sensitivity required for the analysis, and as a result is application specific. While much research has gone into detector development in the last decade, improvement in detector sensitivity is still needed if CE analysis is to become a widely accepted analysis technique, especially in the planar format.

ACKNOWLEDGMENTS

Support for this article was provided by the Welch Foundation (D-1312) and the National Science Foundation (DBI-9876839).

REFERENCES

1. Li, C. and Martin, L. M. *Anal. Biochem.* **1998,** 263, 72.
2. Larive, C. K., Lunte, S. M., Zhong, M., Perkins, M. D., Wilson, G. S., Gokulrangan, G., Williams, T., Afroz, F., Schoeneich, C., Derrick, T. S., Middaugh, C. R., Bogdanowich-Knipp, S. *Anal. Chem.* **1999,** 71, 389R.
3. Nielen, M. W. F. *J. Chromatogra.*, **1993,** 637, 81.
4. Ackermans, M. T., Beckers, J. L., Everaerts, F. M., Hoogland, H., and Tamassen, M. J. H. *J. Chromatogr.* **1992,** 596, 101.
5. Garcia, F. and Henion, J. *J. Chromatogr.* **1992,** 606, 237.
6. Altria, K. D. *LC-GC Int.* **1993,** 6, 616.
7. Altria, K. D. and Rogan, M. M. *J. Pharm. Biomed. Anal.* **1990,** 8, 1000.
8. Altria, K. D. and Rogan, M. M. *Chromatogr. and Anal.* **1994,** April/May, 3.
9. Al-Hakin, A., and Linhardt, R. *J. Anal. Biochem.* **1991,** 199, 241.
10. Damn, J. B. L., Overklift, G. T., Vermeulen, B. W. M., Fluitsma, C. F., and van Dedem, G. W. K. *J. Chromatogr.* **1992,** 608, 297.
11. Ampofo, S. A., Wang, H. M., and Linhardt, R. J. *Anal. Biochem.* **1991,** 199, 249.
12. Chervet, J. P., Van Soest, R. E. J., and Ursem, M. LC Packings, technical communication, **1990.**
13. Mainka, A. and Bachmann, K. *J. Chromatogr.* **1997,** 767, 241.
14. Wang, T., Aiken, J. H., Huie, C. W., and Hartwick, R. A. *Anal. Chem.* **1991,** 63, 1372.
15. Weston, A., Brown, P. R., Jandik, P., Jones, W. R., and Heckenberg, A. L. J. Chromatogr. 1992, 593, 289.
16. Jandik, P. and Jones, W. R. *J. Chromatogr.* **1991,** 546, 431.
17. Heiger, D. N., Kaltenbach, P., Sievert, H-J. P. *Electrophoresis* **1994,** 15, 1234.
18. Hu, T., Zuo, H., Riley, C. M., Stobaugh, J. F., and Lunte, S. M. *J. Chromatogr.* **1995,** 716, 381.

19. Plock, J. and Novotny, M. V. *J. Chromatogr.* **1997,** 757, 215.

20. Jandik, P., Jones, W. R., Weston, A., and Brown, P. R. *LC-GC.* **1991,** 9, 634.

21. Landers, J. P. (editor), *Handbook of Capillary Electrophoresis*, CRC Press, Boca Raton, 1997.

22. Foret, F., Fanali, S., Nardi, A., and Bocek, P. *Electrophoresis*. **1990,** 11, 780.

23. Nielen, M. W. F. *J. Chromatogr.* **1991,** 588, 321.

24. Wang, T. and Hartwick, R. A. *J Chromatogr.* **1992,** 589, 307.

25. Yeung, E. S. *Acc. Chem. Res.* **1989,** 22, 125.

26. Weinberger, R. *Practical Capillary Electrophoresis*. Academic Press, Inc. Boston. 1993.

27. Doble, P., Miroslav, M., and Haddad, P. *J. Chromatogr.* **1988,** 804, 327.

28. Bornhop, D. J. and Dovichi, N. J. *Anal. Chem.* **1987,** 59, 1632.

29. Yu, M. and Dovichi, N. J. *Anal. Chem.* **1989,** 37, 61.

30. Yu, M. and Dovichi, N. J. *Appl. Spectrosc.* **1989,** 43, 196.

31. Waldron, K. C. and Dovichi, N. J. *Anal. Chem.* **1992,** 64, 1396.

32. Earle, C. W. and Dovichi, N. J. *J. Liq. Chromatogr.* **1989,** 12, 1989.

33. Yu, M. and Dovichi, N. J. *Microchem. Acta.* **1988,** III, 27.

34. Chen, M., Waldron, K. C., Zhao, Y., and Dovichi, N. J. *Electrophoresis.* **1994,** 15, 1290.

35. Li, X-F, Liu, C-S, Roos, P, Hansen Jr., E. B, Cerniglia, C. E., and Dovichi, N. J. *Electrophoresis*. **1998,** 19, 3178.

36. Bruno, A. E., Paulus, A., and Bornhop, D. J. *Appl. Spectrosc.* **1991,** 45, 462.

37. Saz, J. M., Krattiger, B., Bruno, A. E., Diez-Masa, J. C., and Widmer, H. M. *J. Chromatogr.* **1995,** 699, 315.

38. Wu, J., Kitamori, T., and Sawada, T. *Anal. Chem.* **1990,** 62, 1676.

39. Wu, J., Odake, T., Kitamori, T., and Sawada, T. *Anal. Chem.* **1991,** 63, 2216.

40. Odake, T., Kitamori, T., and Sawada, T. *Anal. Chem.* **1992,** 64, 2870.

41. Odake, T., Kitamori, T., and Sawada, T. *Anal. Chem.* **1995,** 67, 145.

42. Odake, T., Kitamori, T., and Sawada, T. *Anal. Chem.* **1997,** 69, 2537.

43. Timperman, A. T., Khatib, K, and Sweedler, J. V. *Anal. Chem.* **1995,** 67, 139.

44. Chen, D. Y., Aldelhelm, K., Cheng, X. L., and Dovichi, N. J. *Analyst.* **1994,** 119, 349.

45. Lee, Y-H., Maus, R. G., Smith, B. W., and Winefordner, J. D. *Anal. Chem.* **1994,** 66, 4142.

46. Craig, D. B., Arriaga, E., Wong, J. C. Y., Lu, H., and Dovichi, N. J. *Anal. Chem.* **1998,** 70, 39A.

47. Craig, D. B., Arriaga, E., Wong, J. C. Y., Lu, H., and Dovichi, N. J. *J. Am. Chem. Soc.* **1998,** 118, 5254.

48. Gassman, E., Kuo, J. E., and Zare, R. N. *Science*. **1985,** 230, 813.

49. Chen, D. Y., Swerdlow, H. P., Harke, H. R., Zhang, J. Z., and Dovichi, N. J. *J.Chromatogr.* **1991,** 559, 237.

50. Swerdlow, H., Wu, S., Harke, H., and Dovichi, N. J. *J. Chromatogr.* **1990,** 516, 237.

51. Wu, S. and Dovichi, N. J. *J.Chromatogr.* **1989,** 480, 141.

52. Cheng, Y. F. and Dovichi, N. J. *Science*. **1988,** 242, 562.

53. Kuhr, W. G. and Yeung, E. S. *Anal. Chem.* **1988,** 60, 1832.

54. Kuhr, W. G. and Yeung, E. S. *Anal. Chem.* **1988,** 60, 2642.

55. Shamsi, S. A., Danielson, N. D., and Warner, I. M. *J. Chromatogr.* **1999,** 835, 159.

56. Hernandez, L., Joshi, N., Excalon, J., and Guzman, N. *J. Chromatogr.* **1990,** 502, 247.

57. Hernandez, L., Joshi, N., Excalona, J., and Guzman, N. *J. Chromatogr.* **1991,** 559, 183.

58. Liu, J., Shirota, O., and Novotny, M. *Anal. Chem.* **1991,** 63, 413.

59. Swaile, D. F. and Sepaniak, M. J. *J. Liq. Chromatogr.* **1991,** 14, 869.

60. Nie, S., Dadoo, R., and Zare. N. *Anal. Chem.* **1993,** 65, 3571.

61. Chang, H. T. and Yeung, E. S. *Anal. Chem.* **1995,** 67, 1079.

62. Timperman, A. T., Oldenburg, K. E., and Sweedler, J. V. *Anal. Chem.* **1995,** 67, 3421.

63. McGregor, D. A. and Yeung, E. S. *J. Chromatogr. A.* **1994,** 680, 491.

64. Eriksson, K. O., Palm, A., and Hjerten, S. *Anal. Biochem.* **1992,** 201, 211.

65. Cheng, Y. F., Fuchs, M., Andrews, D., and Carson, W. *J. Chromatogr.* **1992,** 608, 109.

66. Huang, X. and Zare, R. N. *J. Chromatogr.* **1990,** 516, 185.

67. Chen, D. Y. and Dovichi, N. J. *Anal. Chem.* **1996,** 68, 690.

68. Haber, C., Roosli, S., Tsuda, T., Scheidegger, D., Muller, S., and Simon, W. *12th Int. Symp. Capillary Chromatography.* Kobe, Japan, 1990.

69. Haber, C., Silverstri, I., Roosli, S., and Simon, W., *Chimia*. **1991,** 45, 117.

70. Nann, A. and Pretsch, E., *J. Chromotogr.* **1994,** 676, 437.

71. Haung, X., Pang, T. K, Gordaon, M. J., and Zare, R. N. *Anal. Chem.* **1987,** 59, 2747.

72. Huang, X., Gordon, M. J., and Zare, R. N. *J. Chromatogr.* **1988,** 425, 385.

73. Gordon, M. J., Huang, X., Pentoney, S. L., and Zare, R. N. *Science*, **1988,** 63, 224.

74. Reay, J. R., Dadoo, R., Storment, C. W., Zare, R. N., and Kovacs, G. T. A. *Proc. Solid-State Sensore and Actuator Workshop,* Hilton Head, 1994, P. 61.

75. Rosso, T. E. and Bossle, P. C. *J. Chromatogr.* **1998,** 824, 125.

76. Dasgupta, P. K. and Bao, L., *Anal. Chem.* **1993,** 65, 1003.

77. Kar, S., Dasgupta, P. K., Liu, H., and Hwang, H., *Anal. Chem.* **1994,** 66, 2537.

78. Avdalovic, N., Pohl, C. A., Rocklin, R. D., and Stillian, J. R. *Anal. Chem.* **1994,** 66, 2537.

79. Wallingford, R. A. and Ewing, A. G. *Anal. Chem.* **1987,** 59, 1762.

80. Wallingford, R. A. and Ewing, A. G. *Anal. Chem.* **1988,** 60, 1972.

81. Wallingford, R. A. and Ewing, A. G. *J. Chromatogr.* **1988,** 441, 299.

82. Wallingford, R. A. and Ewing, A. G. *Anal. Chem.* **1988,** 60, 258.

83. Ewing, A. G., Wallingford, R. A., and Olefirowicz, R. A. *Anal. Chem.* **1989,** 61, 292A.

84. Olsson, J., Nordstrom, O., Nordstrom, A. C., and Karlberg, B. *J. Chromatogr.* **1998,** 826, 227.

85. Ewing, A. G., Mesaros, J. M., and Gavin, P. F. *Anal. Chem.* **1994,** 66, 527A.

86. O'Shea, T. J., Lunte, S. M, and LaCourse, W. R. *Anal. Chem.* **1993,** 65, 948.

87. Lu, W. Z. and Cassidy, R. M. *Anal. Chem.* **1993,** 65, 2878.

88. Colon, L. A., Dadoo, R., and Zare, R. N. *Anal. Chem.* **1993,** 65, 476.

89. Lin, H., Xu, D. K., and Chen, H. K. *J. Chromatogr.* **1997,** 760, 227.

90. Tarigan, H. J., Neill, P., Kenmore, C. K., and Bornhop, D. J. *Anal. Chem.* **1996,** 15, 1763.

91. Bornhop, D. J. and Dovichi, N. J. *Anal. Chem.* **1986,** 58, 504.

92. Bruno, A. E., Krattinger, B., Maystre, F., Widmer, H. M. *Anal. Chem.* **1991,** 63, 2689.

93. Krattiger, B., Bruno, A. E., Bruin, G. J. *Anal. Chem.* **1994,** 66, 1.

94. Bornhop, D. J. U.S. Patent 5325170, 1994.

95. Bornhop, D. J. *Appl. Opt.* **1995,** 34, 3234.

96. Deng, Y. and Li, B. *Appl. Opt.* **1998,** 37, 998.

97. Wu, J. and Pawliszyn, J. *Anal. Chem.* **1992,** 64, 224.

98. Bruggraf, N., Krattiger, B. de Mello, A., de Rooij, N., and Manz, A. *Analyst.* **1998,** 123, 1443.

99. Buttry, D. A., Vogelmann, T. C., Chen, G., and Goodwin, R. U.S. Patent 5,600,433 , 1997.

100. Born and Wolf, *Principles of Optics*, Pergamon Press, New York, 1975.

101. Saleh, B. E. A. and Teich, M. C. *Fundamentals of Photonics*, Wiley-Interscience, New York, 1991.

102. Swinney, K., Pennington, J., and Bornhop, D. J. *Microchem. J.* **1999,** 62, 154.

103. Swinney, K., Pennington, J., and Bornhop, D. J. *Analyst* 1999, 124, 221.

104. Swinney, K. and Bornhop, D. J. *J. Micro. Column. Sep.* 1999, 11, 596.

105. Chen, C. Y. and Morris, M. D. *Appl. Spec.* 1998, 42, 515.

106. Walker, P. A., III and Morris, M. D. *J. Chromatogr.* 1998, 805, 269.

107. Walker, P. A., III, Kowalchyk, W. K., and Morris, M. D. *Anal. Chem.* **1995,** 67, 4255.

108. Wu, N., Peck, T. L., Webb, A. G., Magin, R. L., and Sweedler, J. V. *Anal. Chem.* **1994,** 66, 3849.

109. Wu, N., Peck, T. L., Webb, A. G., and Sweedler, J. V. *J. Am. Chem. Soc.* **1994,** 116, 7929.

110. Olson, D. L., Peck, T. L., Webb, A. G., and Sweedler, J. V. In *Peptides: Chemistry, Structure, and Biology*, Kaumaya and Hodges, Eds., ESCOM, Leiden, The Netherlands, 730, 1996.

111. Olson, D. L., Lacey, M. E., Webb, A. G., and Sweedler, J. V. *Anal. Chem.* **1999,** 71, 3070.

112. Pentoney, Jr., S. L., Zare R. N., and Quint, J. F. *J. Chromatogr.* **1989,** 480, 259.

113. Pentoney, Jr., S. L., Zare R. N., and Quint, J. F. *Anal. Chem.* **1989,** 61, 1649.